1 **Title**

2 **Methionine coordinates a hierarchically organized anabolic program through *GCN4***

3 Adhish S. Walvekar[1], Rajalakshmi Srinivasan[1], Ritu Gupta[1] and Sunil Laxman[1*]

4 [1] Institute for Stem Cell biology and Regenerative Medicine,

5 NCBS-TIFR campus, GKVK Post, Bellary Road, Bangalore 560065.

6 [*] Correspondence: sunil@instem.res.in

7

8

9 Keywords: methionine, S-adenosyl methionine, Gcn4, growth, pentose phosphate pathway,

10 NADPH, reductive biosynthesis

Abstract

Methionine availability during overall amino acid limitation transforms cells to a proliferative state, the underlying metabolic basis of which remains unclear. Here, we investigate the nature and mechanism of this anabolic transformation, using yeast. Combining comparative transcriptome analysis, biochemical and metabolic flux based approaches, we discover that methionine, predominantly through Gcn4p, controls specific regulatory nodes in metabolism. Methionine increases activity of the pentose phosphate pathway, reductive biosynthetic capacity, and transamination capacity, including the synthesis of glutamate/glutamine. These processes converge on key reactions in the synthesis of costly amino acids, and subsequently nucleotides, which are also induced in a methionine dependent manner. This thereby enables the arrangement of a sequential cascade driving an overall anabolic transformation. Thus, methionine switches cells to anabolism, co-opting a "starvation stress response" regulator, Gcn4p, to achieve this. These results suggest a hierarchical metabolic framework explaining how methionine mediates an anabolic transformation.

Introduction

Cell growth is expensive, and is therefore tightly co-ordinated with the intrinsic cellular metabolic state. Changes in the cellular metabolic state influence global transcription and translation, which determine the cell fate appropriate for that condition (*Broach*, *2012*; *Ljungdahl and Daignan-Fornier*, *2012*; *Dechant and Peter, 2008*; *Brauer et al., 2008*; *Boer et al., 2010*). In general, the enormous metabolic costs incurred during growth and proliferation come from two well-studied phenomena. First, to successfully complete division, a cell must make substantial metabolic investments, in order to replicate its genome, and synthesize proteins, lipids, nucleotides, and other macromolecules. Correspondingly, the

35 process of protein synthesis required for growth itself consumes large amounts of energy
36 (*Warner et al., 2001*; *Warner, 1999*), as the translational output of cells increases (*Jorgensen*
37 *and Tyers, 2004*). Therefore, understanding the key metabolic transformations driving growth
38 are areas of intense study, particularly in cancer biology, ranging from the famous "Warburg
39 effect" (*Warburg, 1956*; *Vander Heiden et al., 2009*), to a broader identification of the
40 biosynthetic and metabolic requirements for cell growth (*DeBerardinis et al., 2008*; *Tong et*
41 *al., 2009*; *Vander Heiden et al., 2009*). However, many fundamental concepts explaining how
42 cell growth and proliferation are coordinated with the metabolic state of a cell remain poorly
43 addressed.

44 Nonetheless, several studies particularly using unicellular models like *Saccharomyces*
45 *cerevisiae* have revealed dedicated strategies utilized by eukaryotic cells to integrate growth
46 with metabolic state (*Brauer et al., 2008*; *Boer et al., 2010*; *Gray et al., 2004*; *Broach, 2012*;
47 *Ljungdahl and Daignan-Fornier*, *2012*; *Cai et al., 2011*; *Slavov and Botstein, 2011*). A
48 powerful approach enabling a systematic dissection of molecular mechanisms and metabolic
49 hierarchies has been to first limit preferred carbon or nitrogen sources, thereby slowing down
50 overall growth. By slowing down overall growth, and then reintroducing individual factors
51 and studying responses, several studies have untangled hierarchies of complex metabolic
52 phenomena, revealed specific nutrient sensing mechanisms in cells, and identified how the
53 build-up and utilization of specific, "sentinel" metabolites control growth outputs (*Brauer et*
54 *al., 2008*; *Boer et al., 2010, 2008*; *Cai et al., 2011*; *Tu et al., 2005, 2007*; *Slavov and Botstein,*
55 *2013*; *Xu et al., 2013*; *Klosinska et al., 2011*; *Laxman and Tu, 2010*; *Sutter et al., 2013*;
56 *Laxman et al., 2013*). Utilizing such a strategy, *S. cerevisiae* subjected to amino acid
57 limitations during a shift from a rich, complex medium with lactate as the carbon source, to a
58 defined minimal medium with the same carbon source, revealed that a single amino acid,
59 methionine (and its metabolite S-adenosylmethionine (SAM)), strongly promoted growth

60 (*Wu and Tu, 2011, Sutter et al., 2013*; *Laxman et al., 2013*; *Laxman et al., 2014*). These
61 observations reinforce a host of data from other eukaryotic systems including mammals
62 suggesting that methionine is a strong growth signal, or "growth metabolite" (*Troen et al.,*
63 *2007*; *Lee et al., 2016, 2014*; *Cavuoto and Fenech, 2012*; *Sugimura et al., 1959*; *Breillout et*
64 *al., 1990*). Therefore, this phenomenon in yeast provides a system using which two
65 fundamental, related questions can be addressed: First, what is the methionine mediated
66 anabolic transformation, and the metabolic logic therein? Second, what is the mechanism by
67 which methionine mediates this anabolic transformation, even in overall amino acid limiting
68 conditions? We address these related questions in this study.

69 Here, building from known models of growth regulation during amino acid limitation,
70 we uncover how methionine uniquely mediates an anabolic transformation. Unexpectedly,
71 methionine availability during challenging nutrient conditions results in cells co-opting
72 Gcn4p, a key mediator of a nutrient stress/survival response, for anabolism. This mediator is
73 necessary for the methionine mediated anabolic transformation, and therefore growth. The
74 methionine mediated anabolic transformation itself is due to an activation of very specific
75 metabolic nodes. When these nodes are coincidently activated, they consequently permit a
76 cascade of events leading to the overall biosynthesis of "costly" amino acids and nucleotides.
77 These results position methionine at an apex of an overall anabolic network, and provide a
78 metabolic logic to how methionine results in cells committing to growth.

Results

Methionine induced growth requires Gcn4p.

When wild-type, prototrophic yeast cells are shifted from a complex, amino acid rich medium with lactate as the sole carbon source (RM), to a synthetic minimal medium containing nitrogen base and lactate (MM), they show a significant lag phase and slower growth (Figure 1A). Supplementation with all 20 standard amino acids restores growth after this nutrient downshift (Figure S1A) (*Sutter et al., 2013*; *Laxman et al., 2014*). Importantly, methionine supplementation alone substantially increases growth (Figure 1A), comparable to or better than adding all eighteen other non-sulfur amino acids (nonSAAs) together (*Sutter et al., 2013*; *Laxman et al., 2014*). Given that methionine is itself not a good "nutrient source", and adding methionine would not transform the medium to a nutrient replete condition, we wondered how methionine might mediate an anabolic and proliferative transformation. We therefore thought that examining key growth/survival regulating nodes that are known to be altered during growth under nutrient stress (in the presence or absence of methionine) might serve as a good starting point from which to address this question. In the currently understood model for cellular responses to amino acid limitation (Figure 1B), the Gcn2p kinase is activated and phosphorylates eukaryotic initiation factor eIF2α. This results in global translational repression, but selective translation of *GCN4* (or Atf4 in mammals), where the Gcn4 protein controls general amino acid biosynthesis (Figure 1B) (*Hinnebusch, 2005*). This process is well conserved across eukaryotes (*Vattem and Wek, 2004*). By monitoring the activity status of these steps within this model, and introducing methionine as a variable, we reasoned that clues might emerge that will lead us to the core metabolic phenomenon regulated by methionine. We therefore monitored outputs of responses during amino acid limitation (illustrated in Figure 1B), to determine if any of these aspects were unusually altered in the presence of methionine.

104 We first monitored global translational output by standard polysome profiling (Figure
105 1C). Expectedly, RM grown cells showed a 3:1 polysome: monosome ratio indicating robust
106 translation, and cells shifted to MM showed a drastic reduction in the polysome pool, and an
107 increased monosome peak (polysome:monosome ratio of ~1:1) (Figure 1C, Figure S1B).
108 Supplementation with either methionine, or all the nonSAAs combined, during the shift to
109 MM also showed an increase in the monosome pool, and a partial restoration of the polysome
110 levels resulting in a polysome: monosome ratio of ~1.7:1 (or ~1.3:1, for nonSAAs) (Figure
111 1C, Figure S1B), suggesting slightly increased translation due to methionine. We also
112 monitored the phosphorylation status of eIF2α (Figure 1D), and expectedly observed a
113 substantial increase in the phosphorylation levels of eIF2α after a RM to MM shift. However,
114 methionine supplementation only marginally reduced the levels of phosphorylated eIF2α, and
115 levels of phosphorylation remained high (Figure 1D). Collectively, the phosphorylation status
116 of the eIF2α, and the results obtained with polysome profiling, suggest that methionine has a
117 modest impact on global translation during amino acid limited growth, but the cells continue
118 to appear "nutrient stressed", while showing increased proliferation. These observations were
119 largely in line with expected outcomes.

120 We next monitored the amounts of endogenous Gcn4p (chromosomally tagged with a
121 C-terminal HA epitope) after a shift to MM, with and without supplementation of different
122 amino acids, expecting a decrease in Gcn4p amounts upon the addition of methionine.
123 Surprisingly, Gcn4p accumulated substantially upon methionine supplementation, compared
124 to MM, or supplementing all 18 other nonSAAs (Figure 1E). This was independently
125 confirmed using immunofluorescence based experiments (Figure S1C). We further asked
126 whether Gcn4p was necessary for the increased growth upon methionine supplementation.
127 Notably, the *gcn4Δ* cells did not show any increased growth in methionine supplemented
128 medium, but instead grew comparably to WT cells growing in MM (Figure 1F). As controls,

129 in all other conditions (lacking methionine, or in RM) the growth of *gcn4Δ* cells was
130 indistinguishable from the WT cells (Figure S1D). Collectively, these data indicate that
131 Gcn4p is necessary uniquely for the methionine-mediated growth in these amino acid poor
132 conditions. Given the established role of Gcn4p as a regulator of metabolic homeostasis, this
133 also suggested that methionine triggered a core transcriptional response, with a key
134 component of this response being mediated by the Gcn4p transcription factor. Thus, we
135 reasoned that dissecting the methionine and Gcn4p mediated transcriptional response might
136 provide insight into the anabolic transformation mediated by methionine, and allow the
137 elucidation of a core metabolic response that drives proliferation.

138

139 **Methionine induces a transcriptional remodelling program driving key anabolic nodes.**

140 These data raise two questions: (i) what is the underlying logic of the anabolic
141 transformation mediated by methionine?, and (ii) what is the contribution of Gcn4p towards
142 this anabolic transformation? We started with a comparative RNA-seq approach in order to
143 address aspects of both questions. In this section we address how methionine transforms cells
144 into an anabolic state. We performed RNA-seq analysis on distinct sample sets of wild-type
145 cells- (i) RM grown, or cells shifted to (ii) MM for 2h, (iii) MM+Met for 2h (Met set), and
146 (iv) MM+nonSAAs for 2h. Transcript reads from the biological replicates showed
147 exceptional correlation across all conditions (Pearson correlation coefficient, $R \geq 0.99$) (Figure
148 S2). Setting a stringent cut-off, we only considered differentially expressed genes with $\geq \log_2$
149 1.5 fold changes, and a p-value cut-off $<10^{-4}$ for further analysis. We first compared global
150 transcription trends in WT cells growing in RM, MM+Met or MM+nonSAAs to MM,
151 focusing on a unique transcriptional signature in the presence of methionine. We examined
152 overall global gene expression trends in these conditions (compared to MM), looking at the

153 distribution of the most induced or downregulated genes (Figure 2A, Figure S3). Strikingly,
154 broad trends of up- or down- regulated genes exhibited by cells in MM+Met were more
155 similar to cells in RM, than the cells in MM+nonSAAs (which were nearly indistinguishable
156 from MM) (Figure 2A, Figure S3 and S4). This suggests that methionine alone is perceived
157 by cells as a stronger "growth cue" than all non-sulfur amino acids combined, and transforms
158 cells into a transcriptional state resembling that of rapidly proliferating cells in complex,
159 amino acid rich media.

160 We next more closely examined the transcriptional response unique to methionine, by
161 comparing transcriptomes of cells growing in MM vs MM+Met (the only variable being
162 methionine). This comparison identified 372 genes, of which 262 genes were upregulated in
163 the +Met set (Figure 2B, Figure S4, Supplementary file E1). Using gene ontology (GO),
164 these genes were grouped into related processes (Figure 2C, Figure S5A, Supplementary file
165 E2). We observed a substantial transcriptional response related to the core translational
166 machinery. Additionally, GO also grouped multiple induced genes into categories that would
167 fit generally under "nucleotide metabolism" (Figure 2C). GO broadly fits these under
168 "purine/pyrimidine" or "nucleobase and nucleotide metabolism", along with the biosynthesis
169 of secondary metabolites (Figure 2C). All of this would be entirely expected for any cell in a
170 proliferative state, since proliferation relies on increased translation and replication. Largely,
171 and unsurprisingly, the GO grouping showed a signature of a cell in a "proliferative state".

172 This form of GO grouping does not lend any insight into the metabolic logic of the
173 methionine mediated response, beyond their obvious requirements for growth. This is largely
174 a limitation of using GO, which builds groups by looking for enriched pathway terms (relying
175 on multiple genes within a pathway to be overrepresented). However, metabolic regulation
176 does not require entire pathways to be regulated, since most regulation happens by
177 controlling key nodes or "rate-limiting steps" in metabolism (*Nelson and Cox, 2017*). We

178 therefore rebuilt connections from metabolic first principles, in order to examine if there were
179 unique nodes that were affected, and to determine if any logical hierarchy of metabolic
180 responses could be built. These groupings will not necessarily be picked up in GO
181 enrichments, but may be central to understanding the metabolic state. By this reconstruction,
182 we compartmentalized the metabolic response regulated by methionine into a group of key
183 biochemical reactions, which could drive (and explain) a majority of the other metabolic
184 processes upregulated (based on gene expression), as described below.

185 Only a few genes involved in classical "carbon/carbohydrate metabolism" were
186 upregulated in the presence of methionine, and strikingly none of them group to glycolysis,
187 the TCA cycle or gluconeogenesis (Figure 2D). Instead, the genes encoding three key
188 enzymes of the pentose phosphate pathway (PPP) (*GND1*, *RKI1* and *TKL1*), which regulate
189 four steps in the PPP, were highly induced in the presence of methionine (Figure 2D).
190 Furthermore, two other genes (*SOL3* and *TAL1*), which control two other steps in the PPP,
191 were also induced by methionine (just below the $\log_2$ 1.5 fold cut-off limit we had arbitrarily
192 set) (Figure 2D). Gnd1p catalyzes the last step in the oxidative arm of the PPP, generating
193 NADPH and producing ribulose-5-phosphate. Most of the genes of the non-oxidative arm of
194 the PPP, which make ribose-5-phosphate and other critical intermediates, are also
195 upregulated (Figure 2D). Additionally, *HXK2*, encoding a hexokinase is highly upregulated
196 when methionine is present. While this is not classified under the PPP (say by GO grouping),
197 this enzyme produces glucose-6-phosphate, which is required as the substrate for the first,
198 rate-limited step of the PPP, so we included it under the PPP in our grouping (Figure 2D).
199 Thus, only the PPP arm of carbon metabolism was induced by methionine. Second, we noted
200 that key regulator resulting in the formation of pyridoxal-5-phosphate or PLP (encoded by
201 *SNO1*), required for all transamination reactions was induced (Figure 2D). Third, transcripts
202 of Gdh1p, which regulates the key nitrogen assimilation reaction resulting in the formation of

203 glutamate (and *GLN1*, which is further required to make glutamine), were highly induced in
204 methionine (Figure 2D). This reaction itself requires NADPH (coming from the PPP, Figure
205 2D), and also is critical for the subsequent formation of all other amino acids, and nucleotides
206 (Figure 2D). Thus, this grouping suggested that methionine induced the PPP-GDH-PLP
207 nodes in metabolism, which could be central for all the downstream anabolic outputs.

208

209 **Methionine sets-up a hierarchical metabolic response leading to anabolism**

210 We therefore inspected the other up-regulated genes that could be grouped broadly
211 under "amino acid biosynthesis", "nucleotide synthesis", and
212 "oxidoreduction/transamination" categories, particularly focusing on the substrates or co-
213 factors required for their function. Notably, essentially all enzymes encoded by these
214 upregulated genes utilized either a PPP intermediate/product, and/or NADPH, and/or
215 glutamate/glutamine, or combinations of all of these (Figure 3A). We next more closely
216 examined the steps in these respective biosynthetic pathways that these genes regulated
217 (coming from Figure 3A), categorizing all steps in the respective amino acid biosynthesis
218 pathway as either the rate-limiting/initiation step and/or final step in the production of that
219 amino acid, organizing them by the use of costly and complex precursors or cofactors (Figure
220 3B). Strikingly, we observed that the methionine induced genes in these pathways regulated
221 the critical, rate-limiting or costly steps in amino acid biosynthesis (p-value of $3.8e^{-09}$,
222 Fisher's exact test), but had little or no significant role in regulating the multiple other genes
223 in the pathway that encode enzymes for the other, inexpensive steps (Figure 3B). Finally,
224 these methionine-induced genes in the "amino acid biosynthesis" bin do not just broadly
225 represent all amino acid biosynthesis, but synthesize what are viewed as the costliest amino
226 acids to synthesize (*Barton et al., 2010*), namely the aromatic amino acids, the branched-

227 chain amino acids, and lysine, which is itself highly overrepresented in ribosomal and core
228 translational machinery proteins (*Laxman et al., 2013*). Similarly, nucleotide biosynthesis
229 involves very large, multi-step pathways. The methionine dependent, upregulated genes
230 encoded enzymes that control only a few of the critical, limiting steps in nucleotide synthesis,
231 and utilize glutamate/glutamine and/or NADPH, as well as pentose sugars from the PPP
232 (Figure 3A). Furthermore, *RNR1*, which encodes the key enzyme in converting
233 ribonucleotides to deoxyribonucleotides (and hence the critical hub for DNA synthesis), is
234 strongly upregulated upon methionine addition (Figure 3A). Separately, we expanded this
235 analysis and compared the methionine response to minimal medium supplemented with all
236 other nonSAAs, and the overall metabolic grouping or organization remained unchanged
237 (Figure S4), with nonSAAs resembling MM. Finally, in MM+nonSAAs, the few highly
238 induced genes (compared to RM) function in methionine (and sulfur-amino acid) related
239 biosynthesis or salvage (Figure S5B, Supplementary file E1), and not additional anabolic
240 reactions. This further supports our overall observations for the role of methionine as an
241 "anabolic signal". Collectively, this comparative transcriptome analysis suggests not just a
242 general anabolic remodelling due to methionine, but a hierarchical metabolic organization
243 induced by methionine (Figure 3C). In this hierarchical organization, methionine induces
244 genes regulating the PPP, key transamination reactions and the synthesis of
245 glutamine/glutamate. These three processes directly allow critical steps in synthesis of the
246 costliest amino acids and nucleotides, and these key steps are also induced by methionine,
247 collectively setting up a structured anabolic program (Figure 3C). These data thus uniquely
248 position methionine as an anabolic cue.

249

250 **Gcn4p regulates the metabolic response due to methionine**

251 We next addressed the contribution of Gcn4p towards this methionine mediated
252 transformation, at the level of transcription. We first examined global trends of gene
253 expression (similar to those in Figure 2A) in the absence of Gcn4p, compared to WT cells.
254 For this, a relative comparison of transcriptomes of *gcn4Δ* cells grown in RM, MM,
255 MM+Met and MM+nonSAAs to wild-type cells in MM was carried out. To our surprise,
256 global gene expression trends in the Met set even more strongly resembled the RM set than
257 WT cells (in methionine, from Figure 2A) (Figure 4A). The transcriptional response in all
258 other conditions was almost unaffected (Figure 4A). This suggested that, unexpectedly, in the
259 absence of *GCN4*, methionine invokes a very strong transcriptional response with global
260 trends seemingly resembling a strong "growth state" (Figure 4A). We more closely compared
261 transcriptomes of WT cells with *gcn4Δ* cells, under the same combination of conditions used
262 earlier, and analyzed our data with the same stringent filters used in the previous section. The
263 overall changes in transcriptomes of WT vs *gcn4Δ* cells are shown (Figure 4B, Figure S6,
264 Supplementary file E1). Notably, in all other conditions except methionine, WT and *gcn4Δ*
265 cells showed similar gene expression profiles (Figure 4B). To dissect the role of Gcn4p in the
266 methionine response, we compared relative transcript amounts, for the transcripts induced by
267 methionine, in cells lacking Gcn4p compared to MM. When grouped using GO, we found
268 that a very large number of genes (~200) induced in the presence of methionine, grouped into
269 the general groups of "ribosome/translation", and "nucleotide synthesis" (Figure 4C,
270 Supplementary file E2). Again, this representation was even more striking than that seen in
271 WT cells (Figure 2C), suggesting a strong "growth signature" in the presence of methionine
272 in cells lacking Gcn4p.

273 Note that (as shown earlier in Figure 1F) Gcn4p was essential for the growth
274 induction due to methionine. These data therefore paradoxically suggested that the overall
275 "growth signature" response due to methionine was being amplified in the absence of Gcn4p,

276 which might mean that Gcn4p only directly regulated a small number of critical steps in this
277 growth program. We therefore more carefully compared transcript amounts from WT and
278 *gcn4Δ* cells, growing in the presence of methionine (+met), and separated our functional
279 groupings (based on GO) into two broad "bins". One bin represented all genes related to
280 ribosome function and translation (as seen in Figure 2C), while the other bin included the
281 core metabolic genes (similar to those in Figures 2 and 3) (Figure 4D). Strikingly, transcripts
282 of every gene that mapped to ribosome/translation function (from Figure 2C) was higher in
283 *gcn4Δ* cells compared to WT cells in the presence of methionine (Figure 4D). Contrastingly,
284 every gene related to amino acid biosynthesis (and related metabolism) was significantly
285 lower in the *gcn4Δ* cells (Figure 4D). Thus, this organization revealed that in the presence of
286 methionine, while the induction of the translation machinery, and many "nucleotide
287 synthesis" genes was not Gcn4p- dependent, the entire core metabolic transformation might
288 hinge upon Gcn4p.

289 Therefore, we carefully examined the methionine- and Gcn4p- dependent
290 transcription of genes that functionally regulated the PPP, key transamination reactions, or
291 the specific nodes in amino acid biosynthesis (Figure 4E). Strikingly, the genes from the PPP,
292 and transamination reactions were strongly downregulated in *gcn4Δ* cells compared to WT
293 cells in methionine (Figure 4E). Gdh1 (required for glutamate synthesis) was induced by
294 methionine, but was not Gcn4p dependent (Figure 4E). Next, the transcripts of genes
295 encoding key, rate-limiting steps in multiple branched-chain or aromatic amino acid, and
296 lysine and arginine biosynthesis were induced by methionine in a Gcn4p-dependent manner
297 (Figure 4). Finally, while most nucleotide biosynthesis genes were not Gcn4p- dependent, the
298 entire RNR complex (critical for NTP to dNTP conversion) was strongly methionine- and
299 Gcn4p- dependent (Figure 4E). Collectively, these data suggest that the anabolic program
300 induced by methionine requires Gcn4p.

301

302 **Methionine stimulates key transamination and reductive biosynthetic processes in**
303 **amino acid biosynthesis.**

304 We therefore wanted to more directly examine the extent of (i) methionine controlling
305 this anabolic transformation, through the PPP, reductive biosynthesis coupled reactions,
306 transamination reactions and glutamine/glutamate synthesis feeding subsequent amino acid,
307 cofactor, or nucleotide synthesis; and (ii), the extent of Gcn4p dependence for these steps.
308 We first tested these possibilities at the biochemical level, comparing the actual enzyme
309 amounts of three key targets that represent the coupling of the PPP with other processes.
310 These are Snz1p, Gnd2p and Gdh1p. Snz1p is required for pyridoxal phosphate (PLP)
311 biosynthesis (*Dong et al; 2004*), and PLP is essential for all transamination reactions (*Nelson*
312 *and Cox, 2017*). As illustrated earlier in Figure 2D, PLP biosynthesis itself requires the PPP
313 intermediate erythrose-4-phosphate as a substrate. Gnd2p is the key NADPH generating
314 enzyme in the oxidative branch of the PPP. Gdh1p consumes NADPH and makes glutamate
315 from 2-ketoglutarate. We measured amounts of these enzymes from WT and *gcn4Δ* cells
316 growing in MM, and MM+methionine (Figure 5A). Notably, Snz1p and Gnd2p showed a
317 strong induction requiring both methionine and Gcn4p (Figure 5A, Figure S7). Gdh1p was
318 strongly dependent upon methionine, but was not on Gcn4p (Figure 5A). We next measured
319 *in vitro* Gdh1p activity (NADPH-GDH activity) in lysates from cells growing in MM or with
320 methionine, and found that overall Gdh1p activity was higher in cells growing with
321 methionine (Figure 5B). However, as seen in the Western blot analysis (Figure 5A), the *in*
322 *vitro* Gdh1p activity was not dependent on Gcn4p (not shown). These data support the
323 observation that methionine drives these key, coupled steps in biosynthesis, and that they are
324 largely mediated by Gcn4p. Finally, an expected crude readout of this biochemical coupling

should be changes in steady-state nucleotide amounts, requiring Gcn4p in methionine replete conditions. Comparing relative amounts of nucleotides in wild-type and *gcn4Δ* cells, we noted a decrease in the nucleotide amounts in *gcn4Δ* cells in the presence of methionine (Figure 5C). Collectively, direct, steady-state biochemical read-outs support the hypothesis emerging from the transcriptional response seen to methionine, suggesting a coupled regulation of the PPP, and key transamination reactions, leading to increased amino acid and nucleotide synthesis.

Methionine stimulates *de novo* biosynthesis of key amino acids in a Gcn4p- dependent manner.

Validating these findings using metabolite measurements is challenging, since any steady-state metabolite measurement (as in Figure 5C) will undoubtedly show differences between cells, but cannot directly distinguish synthesis from consumption. Therefore, to directly resolve this, we resorted to a stable-isotope based pulse labelling and LC-MS/MS based approach to directly measure the new synthesis of amino acids. To WT or *gcn4Δ* cells in the respective medium with or without methionine, we pulsed ^{15}N labelled ammonium sulfate, and measured the ^{15}N incorporation into amino acids (Figure 6A, Table S2), before an effective "steady-state" of labelled amino acid synthesis and consumption was reached. This will permit the detection of newly synthesized amino acids, which will have incorporated the ^{15}N label, before a steady-state is reached. We observed that biosynthesis of all the aromatic amino acids, lysine, histidine, proline, arginine and asparagine is strongly dependent on methionine (Figure 6B). For technical reasons it was not possible to measure label-incorporation into branched-chain amino acids. Notably, the label immediately percolated in asparagine and aromatic amino acid biosynthesis, and showed a very strong

349 methionine dependence (Figure 6B). Asparagine, proline and phenylalanine biosynthesis
350 were methionine dependent even in *gcn4Δ* cells, pointing towards some *GCN4*-independent
351 roles of methionine. For all the other amino acids measured, their biosynthesis increased in
352 the presence of methionine in a *GCN4*-dependent manner (Figure 6B). These data directly
353 validate our earlier observations, strongly suggesting that methionine availability controls the
354 key nodes around PPP-PLP-GDH axis thereby generating the amino acid pool required for
355 proliferation.

356

357 **Methionine increases nucleotide biosynthesis in a Gcn4p- dependent manner.**

358 Given that the PPP and amino acid biosynthesis (leading to nucleotide biosynthesis)
359 are directly regulated by methionine and Gcn4p, we predicted that collectively, perturbing
360 this node should have a severe consequence on nucleotide biosynthesis, even if most
361 nucleotide biosynthesis genes themselves were not regulated by Gcn4p. We therefore adopted
362 a direct, quantitative estimation of methionine and Gcn4p dependent increases in nucleotide
363 synthesis (similar to the approach in Figure 6). This would directly reflect flux through the
364 coupled steps of the PPP, glutamate/glutamine synthesis, and the use of intermediates from
365 amino acid biosynthetic pathways for carbon and nitrogen assimilation into nucleotides
366 (Figure 7A). The carbon skeleton of nucleotides comes from the PPP, the nitrogen base is
367 directly derived from glutamine/glutamate and aspartate, and glutamate synthesis is itself
368 coupled to NADPH (from the PPP) (Figure 7A). Furthermore, nucleotide biosynthesis is also
369 coupled to histidine and tryptophan synthesis. Using a stable-isotope based nitrogen or
370 carbon pulse labelling approach, coupled to targeted LC-MS/MS based measurement of
371 nucleotides, we separately measured the incorporation of the nitrogen and carbon label into
372 nucleotides, to estimate newly synthesized nucleotides before homeostasis was reached, as

373 illustrated in Figure 7B and 7C. We observed a dramatic increase in ^{15}N-labelled nucleotides
374 upon the addition of methionine (Figure 7B, Table S2). Furthermore, this methionine-
375 mediated incorporation of ^{15}N-label in nucleotides was entirely Gcn4p- dependent (Figure 7B
376 and Figure S8). Monitoring carbon flux is extremely challenging in a non-fermentable carbon
377 source like lactate (as compared to glucose), given the difficulties of following the labelled
378 carbon molecules. Despite that, like the ^{15}N-labeling experiments described above, a similar
379 experimental design of 0.5X-label spiking was adopted to measure the ^{13}C-label
380 incorporation into AMP (Figure 7C, Table S2). We observed a significant increase in ^{13}C-
381 labelled AMP upon the addition of methionine, and this methionine dependent incorporation
382 of ^{13}C-label in AMP was not observed in cells lacking Gcn4p (Figure 7C). Collectively, this
383 shows a methionine and Gcn4p dependent increase in *de novo* synthesis of nucleotides,
384 coupling carbon and nitrogen flux that is dependent on the PPP, and glutamate synthesis.

385 **Discussion**

386 In this study, we show how methionine availability drives cellular proliferation
387 through an anabolic transformation, even under amino acid limited, apparently challenging
388 conditions. We uncover a regulated, hierarchical activation of metabolic processes in the
389 presence of methionine, which lead to an anabolic state. We also provide a mechanism of
390 how methionine mediates this anabolic transformation.

391 Starting with a framework of existing models for responses to amino acid limitation,
392 we find that the overall methionine mediated growth depends upon Gcn4p (Figure 1).
393 Surprisingly, methionine results in increased Gcn4p, and Gcn4p is necessary for the
394 methionine mediated anabolic transformation (Figure 1). More pertinently, methionine,
395 substantially through Gcn4p, mediates a transcriptional remodelling in cells controlling the
396 anabolic transformation, and not the translation component (Figures 2, 4). Understanding the
397 core metabolic logic within the transcriptional response to methionine required a
398 reorganization of GO based groupings based on metabolic first principles, and the logic that
399 emerged was striking (Figure 2, 3 and 4). Methionine positively regulates the pentose
400 phosphate pathway (PPP) (Figure 2). The PPP provides the pentose sugar backbones for
401 nucleotides, along with reducing equivalents (NADPH) allowing reductive biosynthesis for a
402 variety of anabolic molecules (*Nelson and Cox, 2017*). Key among these are amino acids and
403 nucleotides. For amino acid and nucleotide synthesis, pyridoxal phosphate, which controls all
404 transamination reactions, is essential (*Eliot and Kirsch, 2004*) (Figure 2). Notably, genes
405 controlling these three key nodes in metabolism are all strongly induced by methionine
406 (Figure 2). These steps feed the subsequent metabolic nodes induced by methionine.
407 Methionine induces the expression of genes that control rate limiting or final steps in the
408 synthesis of "costly" amino acids, the aromatic amino acids and the branch chain amino acids
409 (Figure 3). Almost every one of these (methionine regulated) steps use cofactors or

410 intermediates from the pentose phosphate pathway, are transamination reactions requiring
411 PLP, or/and require glutamate or glutamine (which depends on the PLP mediated
412 transamination) (Figure 2 and 3). Thus, it appears that methionine sets up this metabolic
413 hierarchy, as illustrated in a schematic in Figure 3C and 7D. Interestingly, the methionine-
414 induced activity in most of these metabolic nodes, and thus the overall anabolic
415 transformation, depends upon Gcn4p (Figure 4). Gcn4p is best understood as a regulator of
416 amino acid biosynthesis during starvation (*Natarajan et al., 2001*). However, while many of
417 the *GCN4* targets picked up in our study compare well with the landmark study of *GCN4*
418 targets (*Natarajan et al., 2001*) (see Figure S9 and Table S3), the role of Gcn4p in the
419 presence of methionine in controlling these key hubs of the PPP, glutamate biosynthesis, and
420 rate regulating steps in costly amino acid and nucleotide biosynthesis has not been previously
421 appreciated, particularly in contexts where growth is enhanced. A combination of rigorous
422 biochemical, and metabolic flux based analysis using stable-isotopes directly demonstrate
423 this coupling of the PPP, NADPH utilization and transamination reactions (in both nitrogen
424 assimilation and carbon assimilation) first towards the increased synthesis of aromatic and
425 branch-chain amino acids, and next towards nucleotides, in a methionine- and Gcn4p-
426 dependent manner (Figures 6, 7). Interestingly, Gcn4p appears to regulate only the core
427 metabolic program induced by methionine, and not the induction in the synthesis of the
428 translation machinery (as seen in Figure 4). Collectively, our data not just shows how
429 methionine can co-opt Gcn4 to achieve a "growth state", but suggests how methionine sits
430 atop a pyrimidical hierarchy of metabolic events, that set up an anabolic transformation
431 (model in Figure 3C).

432 The central role of the PPP in anabolism is now text-book knowledge (*Nelson and*
433 *Cox, 2017*). Yet, a better appreciation of the importance of the PPP in mediating anabolic and
434 proliferative transformations is now emerging due to the association of the PPP to cancer

435 metabolism (*Patra and Hay, 2014*; *Cairns et al., 2011*). Many anabolic transformations
436 require contributions from the PPP, however, the metabolic cues regulating the PPP (and
437 coupling to other processes) are not often obvious. More generally, our study highlights how
438 methionine (likely through its downstream metabolite SAM), acts as an anabolic signal for
439 cells. This is analogous to another central metabolite, acetyl-CoA, better known to determine
440 cellular decisions towards growth (*Cai et al., 2011*; *Comerford et al., 2014*; *Shi and Tu, 2013*;
441 *Pietrocola et al., 2015*; *Mariño et al., 2014*). Interesting correlations can be made from our
442 observations to known roles of methionine in cancer cell metabolism, and metazoan growth.
443 The earliest observations of methionine as important for some cancers to proliferate dates
444 back to the 1950s (*Cavuoto and Fenech, 2012*; *Sugimura et al., 1959*; *Breillout et al., 1990)*,
445 and several types of cancer cells are addicted to methionine (*Halpern et al., 1974*; *Stern and*
446 *Hoffman, 1986*; *Guo et al., 1993*; *Lu and Epner, 2000*; *Poirson-Bichat et al., 2000*;
447 *Kokkinakis et al., 2001*; *Cellarier et al., 2003*; *Cavuoto and Fenech, 2012*; *Clarke et al.,*
448 *2016*). Other, distinct studies show that *Drosophila* fed on methionine rich diets exhibit rapid
449 growth, high fecundity, and shorter lifespans (*Troen et al., 2007*; *Lee et al., 2016, 2014*), all
450 hallmarks of what a "proliferative" metabolite will do. Studies from yeast show how
451 methionine inhibits autophagy, or regulates the TORC1 to boost growth (*Sutter et al., 2013*;
452 *Laxman et al., 2013, 2014*). One of the earliest known cell cycle entry check-points is linked
453 to methionine (*Unger and Hartwell, 1976*). Upon sulfate (and thereby methionine) starvation,
454 cells arrest their growth to promote survivability (*Boer et al., 2008*), and transform their
455 proteome to preferentially express proteins containing fewer cysteine/methionine residues to
456 save sulfur (*Fauchon et al., 2002*). There are other, less appreciated observations connecting
457 methionine metabolism and the pentose phosphate pathway. Yeast cells lacking *ZWF1*
458 (encoding glucose-6-phosphate dehydrogenase, the first enzyme in the PPP) exhibit
459 methionine auxotrophy (*Thomas et al., 1991*), and methionine supplementation increases the

460 oxidative stress tolerance of *zwf1Δ* (*Campbell et al., 2016*). While these studies highlight this
461 critical role of methionine in anabolism, an overarching logic of the core anabolic
462 transformation mediated by methionine, and the mechanisms by which this is mediated, have
463 remained unclear. Our study directly elucidates this.

464 Note that our study emphasizes the use of prototrophic ("wild type") yeast strains to
465 study responses to amino acids. Typically, studies utilize laboratory strains derived from an
466 auxotrophic backgrounds (eg. S288C/BY4741), which require supplemented uracil, histidine,
467 leucine and methionine for survival (*Sherman, 1991*; *Pronk, 2002*; *Corbacho et al., 2011*;
468 *Brachmann et al., 1998*; *Gerashchenko and Gladyshev, 2014*; *Alam et al., 2016*). This
469 precludes experiments in amino acid limitation. Additionally, our use of a "less-preferred"
470 carbon source, lactate, can help reveal regulatory phenomena otherwise hidden in glucose and
471 amino acid rich laboratory conditions, where a surfeit of costly metabolic resources are
472 present. Notably, several recent reports emphasize the importance of lactate as a carbon
473 source in rapidly proliferating cells (*Kennedy et al., 2013*; *Faubert et al., 2017*; *Hu et al.,*
474 *2017*), and our observations provide mechanistic and molecular insight into growth under
475 these conditions. Finally, the so called integrated stress response (ISR), and the Gcn4p
476 ortholog in mammals, Atf4, play important roles in cancer cell proliferation (*Bi et al., 2005*;
477 *Ye et al., 2010*; *Palam et al., 2015*), and many cancers continue to grow in apparently poor
478 nutrient environments. Our study suggests how, in methionine rich (but otherwise amino acid
479 limiting) conditions, Gcn4/Atf4 could function to promote growth, and not just help cells
480 recover from nutrient stress. A separate emerging question will be to understand how Gcn4p
481 is itself regulated under these otherwise amino acid limited conditions, by methionine.

482 We close by reiterating a possible metabolic cost based hypothesis for what might
483 make methionine a strong growth cue. The *de novo* synthesis of methionine and its
484 immediate metabolites (notably SAM) is exceptionally costly in terms of NADPH molecules

485 invested (*Thomas and Surdin-Kerjan, 1997*; *Kaleta et al., 2013*; *Mampel et al., 2005*; *Sutter*
486 *et al., 2013*). Cells require at least 6 molecules of NADPH to reduce sulfur to synthesize a
487 single molecule of methionine. Since biology has tied multiple anabolic processes to
488 reductive biosynthesis (dependent on NADPH from the PPP), the availability of methionine
489 might be an ancient signal to represent a metabolic state where reductive equivalents are
490 sufficiently available for all other reductive biosynthetic processes as a whole.

491

492 **Materials and Methods:**

493 **Yeast strains and growth media**

494 The prototrophic CEN.PK strain (referred to as wild type, WT) was used in all experiments
495 (*van Dijken et al., 2000*). Strains with gene deletions or chromosomally tagged proteins (at
496 the C-terminus) were generated as described. Strains used in this study are listed in Table S1.

497 The growth media used in this study are RM (1% yeast extract, 2% peptone and 2% lactate)
498 and MM (0.17% yeast nitrogen base without amino acids, 0.5% ammonium sulfate and 2%
499 lactate). All amino acids were supplemented at 2 mM. NonSAAs refers to the mixture of all
500 standard amino acids (2 mM each) except methionine, cysteine and tyrosine.

501 The indicated strains were grown in RM with repeated dilutions (~36 hours), and the culture
502 in the log phase (absorbance at 600 nm of ~1.2) was subsequently switched to MM, with or
503 without addition of the indicated amino acids. For growth curves, the RM acclimatized
504 cultures were used and diluted in a fresh medium with the starting absorbance of ~0.2 and the
505 growth was monitored at the indicated time intervals.

506 **Polysome analysis**

507 The cells (50 OD) were treated with cycloheximide (100 µg/ml) for 15 minutes before
508 harvesting in ice-filled, cold centrifuge bottles. The pellet obtained after centrifugation
509 (8000g, 5 min, 4°C) was once washed, and then re-suspended in 0.5 ml lysis buffer (10 mM
510 Tris-HCl pH 7, 0.1 M NaCl, 30 mM $MgCl_2$, 1U/µl Ribolock RNase inhibitor and 80 µg/ml
511 cycloheximide) with chilled, baked acid-washed glass beads. After bead-beating, 0.5 ml lysis
512 buffer was added and the crude extract obtained was centrifuged (18407g, 10 min, 4°C) and
513 the supernatant (200 µl) containing polysomes is fractionated on a sucrose gradient (7%-47%
514 sucrose; containing 20 mM Tris-HCl pH 7, 140 mM KCl, 5 mM $MgCl_2$, 1 mM DTT and 50

515 μg/ml cycloheximide) by ultra-centrifugation (35000 rpm, 3 h, 4°C). The polysome profile
516 was obtained on an ISCO fractionator, wherein the absorbance at 254 nm was traced. For
517 polysome: monosome ratio calculation, area under the curve was quantified using ImageJ
518 software (*Rasband, ImageJ*, U. S. National Institutes of Health, Bethesda, Maryland, USA,
519 http://imagej.nih.gov/ij/, 1997-2016).

520 **Western blot analysis**

521 Approximately ten OD_{600} cells were collected from respective cultures, pelleted and flash-
522 frozen in liquid nitrogen until further use. The cells were re-suspended in 400 μl of 10%
523 trichloroacetic acid and lysed by bead-beating three times: 30 sec of beating and then 1 min
524 of cooling on ice. The precipitates were collected by centrifugation, re-suspended in 400 μl of
525 SDS-glycerol buffer (7.3% SDS, 29.1% glycerol and 83.3 mM Tris base) and heated at
526 100°C for 10 min. The supernatant after centrifugation was treated as the crude extract.
527 Protein concentrations from extracts were estimated using bicinchoninic acid assay (Thermo
528 Scientific). Equal amounts of samples were resolved on 4 to 12% Bis-Tris gels (Invitrogen).
529 Coomassie blue–stained gels were used as loading controls. Western blots were developed
530 using the antibodies against the respective tags. We used the following primary antibodies:
531 monoclonal FLAG M2 (Sigma), HA (12CA5, Roche), and phosphor-eIF2α Ser51 (9721, Cell
532 Signaling). Horseradish peroxidase–conjugated secondary antibodies (mouse and rabbit)
533 were obtained from Sigma. For Western blotting, standard enhanced chemiluminescence
534 reagents (GE Healthcare) were used. ImageJ was used for quantification.

535 **Immunofluorescence measurements**

536 Yeast cells were fixed with 3.7% formaldehyde, washed and resuspended in spheroplasting
537 buffer (40 mM potassium phosphate buffer, pH 6.5; 0.5 mM $MgCl_2$; 1.2 M sorbitol).
538 Spheroplasts were prepared by zymolyase (MP Biomedicals, 08320921) treatment and spread

539 on a slide pretreated with 50 µl of 1 mg/ml polylysine (Sigma-Aldrich, P6407). Gcn4-HA
540 was stained with the mouse monoclonal anti-HA (12CA5) primary antibody (Roche,
541 11583816001) and Alexa Fluor 488-conjugated Goat anti-Mouse IgG (H+L) secondary
542 antibody (Thermofisher, A32723). DNA was stained with 1µg/ml DAPI for 2 minutes,
543 washed and mounted in Fluoromount-G (Southern Biotech, 0100-01). The cells were imaged
544 using Olympus FV1000 confocal microscope.

545 **RNA-seq analysis**

546 Total RNA from yeast cells was extracted using hot acid phenol method (*Collart and*
547 *Oliviero, 2001*). The quality of RNA was checked on Bioanalyzer using an RNA 6000 Nano
548 kit (Agilent) and the libraries were prepared using TruSeq RNA library preparation kit V2
549 (Illumina). The samples were sequenced on Illumina platform HiSeq2500. The raw data is
550 available with NCBI-SRA under the accession number SRP101768. Genome and the
551 annotation files of *S. cerevisiae* S288C strain were downloaded from Saccharomyces
552 Genome Database (SGD; http://www.yeastgenome.org/). 100-mer, single-end reads obtained
553 from RNA sequencing experiments were mapped to the S288C genome using Burrows
554 Wheeler Aligner (BWA) (*Li and Durbin, 2009*). Mapped reads with the mapping quality of ≥
555 20 were used for the further analysis. The number of reads mapped to each gene was
556 calculated and the read count matrix was generated. The read count matrix was fed into
557 EdgeR, a Bioconductor package used for analyzing differential gene expression (*Robinson et*
558 *al., 2010*). Genes which are differentially expressed by at least 3-fold with the p-value of
559 <0.0001 were considered for further analysis. Normalized gene expression was calculated by
560 dividing the number of reads by the gene length and the total number of reads for those
561 samples, then dividing each of these values with the mode of its distribution (*Srinivasan et*
562 *al., 2013*). Absolute expression levels of the genes between the replicates are well correlated
563 with the Pearson correlation coefficient (R) values more than 0.99 (see Figure S2). Mapping

564 of genes to the related pathways and gene ontology analysis were carried out using public
565 databases such as Yeastcyc (*Caspi et al., 2014*), GeneCodis (*Tabas-Madrid et al., 2012*;
566 *Nogales-Cadenas et al., 2009*; *Carmona-Saez et al., 2007*) and SGD (*Dwight et al., 2002*).

567 **Metabolite extractions and measurements by LC-MS/MS**

568 Cells were grown in RM for ~36 hours and transferred to MM with and without methionine
569 for the indicated time. After incubation, cells were rapidly harvested and metabolite extracted
570 as described earlier (*Tu et al., 2007*). Metabolites were measured using LC-MS/MS method
571 as described earlier (*Laxman et al., 2014*). Standards were used for developing multiple
572 reaction monitoring (MRM) methods on Thermo Scientific TSQ Vantage triple stage
573 quadrupole mass spectrometer or Sciex QTRAP 6500. For positive polarity mode,
574 metabolites were separated using a Synergi 4µ Fusion-RP 80A column (150 × 4.6 mm,
575 Phenomenex) on Agilent's 1290 infinity series UHPLC system coupled to mass spectrometer.
576 Buffers used for separation were: buffer A: 99.9% H_2O/0.1% formic acid and buffer B:
577 99.9% methanol/0.1% formic acid (Flow rate, 0.4 ml/min; T = 0 min, 0% B; T = 3 min, 5%
578 B; T = 10 min, 60% B; T = 10.1 min, 80% B; T = 12 min, 80% B; T = 14 min, 5% B; T = 15
579 min, 0% B; T = 20 min, stop). For negative polarity mode, metabolites were separated using
580 a Luna HILIC 200A column (150 × 4.6 mm, Phenomenex). Buffers used for separation were:
581 buffer A: 5 mM ammonium formate in H_2O and buffer B: 100% acetonitrile (flow rate: 0.4
582 ml/min; T = 0 min, 95% B; T = 1 min, 40% B; T = 7 min, 10% B; T = 11 min, 1% B; T = 13
583 min, 95% B; T = 17 min, stop). The area under each peak was calculated using Thermo
584 Xcalibur software (Qual and Quan browsers).

585 **^{15}N- and ^{13}C- based metabolite labelling experiments**

586 For detecting ^{15}N-label incorporation in amino acids and nucleotides, ^{15}N-ammonium sulfate
587 with all nitrogens labelled (Sigma- Aldrich) was used. For ^{13}C-labeling experiment, ^{13}C-

588 lactate with all carbons labelled (Cambridge Isotope Laboratories) was used. In the labelling
589 experiments, 0.5X refers to 0.25% ammonium sulfate or 1% lactate. All the parent/product
590 masses measured are enlisted in Table S2. Amino acid measurements were done in the
591 positive polarity mode. For all the nucleotide measurements, release of the nitrogen base was
592 monitored in positive polarity mode. For the ^{13}C-label experiment, the phosphate release was
593 monitored in negative polarity mode. Under these conditions, the nitrogen base release cannot
594 be monitored here as the nitrogen base itself has carbon skeleton, which will complicate the
595 analysis. The HPLC and MS/MS protocol was similar to those explained above.

596 **GDH assays**

597 Glutamate dehydrogenase activity was measured as described in (*Doherty, 1970*), with some
598 modifications. Yeast cells were lysed by bead-beating in lysis buffer (100 mM potassium
599 phosphate buffer, pH 7; 5% glycerol; 1 mM PMSF; 0.1% Tween-20; 1 mM EDTA; 1 mM 2-
600 mercaptoethanol). NADP-dependent activity was measured by monitoring oxidation of
601 NADPH (assay buffer: 100 mM Tris-HCl, pH 7.2; 10 mM 2-ketoglutarate, pH adjusted to
602 7.2; 100 mM ammonium chloride; 0.1 mM NADPH) at 340 nm. Protein concentrations from
603 extracts were estimated using bicinchoninic acid assay (Thermo Scientific). One enzyme unit
604 corresponds to the amount of enzyme required to oxidize one μmol of NADPH min^{-1} at room
605 temperature.

606 **Statistical analysis**

607 In most of the experiments, Student's t-test was applied for calculating the p-values.
608 Wherever necessary, other tests were applied and indicated accordingly.

609 **Acknowledgements:**

610 We acknowledge Dhananjay Shinde, Padma Ramakrishnan and the NCBS/inStem/C-CAMP
611 Mass spectrometry facility for LC-MS/MS support, Avadheesh Pandit and the
612 NCBS/inStem/C-CAMP next-generation sequencing facility for assistance with library
613 preparation, and Ravi Muddashetty for the polysome fractionator. We thank Utpal Banerjee,
614 Mark Sharpley, Marco Foiani, Christopher Bruhn, Krishnamurthy Natarajan and PJ Bhat for
615 critical comments on this manuscript. This work was supported by a Wellcome Trust-DBT
616 IA intermediate fellowship (IA/I/14/2/501523) and inStem/DBT institutional support to SL.
617 ASW, RG, RS acknowledge bridging fellowships (from inStem), and ASW, RG and RS are
618 supported by DST SERB-national postdoctoral fellowships (PDF/2015/000225,
619 PDF/2016/000416 and PDF/2016/001877 respectively).

620 **Figure legends:**

621 **Figure 1: Methionine induced growth requires Gcn4p.**

622 A) Methionine and growth during amino acid limitation. Shown are growth profiles of WT
623 cells grown in RM and shifted to MM with or without the indicated amino acid supplements
624 (2 mM each; nonSAAs indicates all the non-sulfur amino acids except tyrosine). The growth
625 profile with methionine is in blue. Also see Figure S1A.

626 B) The current model explaining cellular responses to amino acid starvation. Amino acid
627 starvation activates the Gcn2p kinase, leading to decreased levels of the ternary complex. The
628 key outputs indicating amino acid starvation (highlighted in green) are increased
629 phosphorylation of eIF2α, global translational repression, and induced Gcn4p translation.

630 C) Global translational repression is moderately rescued by methionine. WT cells were
631 grown to mid-log phase in RM and shifted to MM, MM plus methionine or MM plus
632 nonSAAs for two hours. The cells were treated with cycloheximide for 15 min before
633 harvesting and polysome pool was fractionated on sucrose gradients using
634 ultracentrifugation. The polysome/monosome ratio for the corresponding samples is shown.
635 Also see Figure S1B.

636 D) Methionine and eIF2α phosphorylation. Yeast cells grown in RM were shifted to the
637 indicated media. The samples were analysed for phosphorylation status of eIF2α (Sui2p in
638 yeast) by Western blot. Rapamycin (100 nM) treated cells served as a positive control. WT
639 cells expressing FLAG-tagged eIF2α were used to monitor the protein abundance under
640 identical conditions. A representative blot is shown.

641 E) Gcn4p amounts in the presence of methionine during amino acid limited growth. Gcn4p
642 was detected by Western blotting of WT cells (expressing Gcn4p with an HA epitope, tagged
643 at the endogenous locus) shifted from RM to MM, or MM supplemented with the indicated
644 combinations of amino acids. RM grown cells treated with rapamycin (100 nM) served as a
645 positive control for Gcn4p induction. A representative blot is shown.

646 F) *gcn4Δ* cells and methionine-mediated growth. The WT and *gcn4Δ* strains were shifted
647 from RM to MM with or without methionine supplementation and growth was monitored.
648 Also see Figure S1D.

649 In all panels, data shows mean±SD. $^{*}p < 0.05$.

650

651 **Figure 2: Methionine induces a transcriptional remodelling program driving key**
652 **anabolic nodes.**

653 A) Global trends of gene expression in RM and methionine supplemented MM. Boxplot
654 shows gene expression levels of transcripts in WT cells grown in RM, or shifted to MM plus
655 methionine, or MM plus nonSAAs in comparison to MM set.

656 B) Effect of methionine on a transcriptional program in cells. The heat map shows
657 differentially expressed genes in MM plus methionine and MM plus nonSAAs compared to
658 MM set.

C) GO analysis of the methionine-responsive genes. The pie-chart depicts the processes grouped by GO analysis for the up-regulated transcripts between MM plus methionine and MM set. Numbers in the bracket indicate the number of genes from the query set/ total number of genes in the reference set for the given GO category.

D) Manual regrouping of the methionine responsive genes into relevant metabolic pathways, focusing on carbon metabolism and central metabolic processes. The pathway map includes individual genes in central carbon metabolism which are induced by methionine (indicating the fold-changes in gene expression). The arrows marked red indicate increased expression across the pathway.

Figure 3: Methionine sets-up a hierarchical metabolic response leading to anabolism.

A) Regrouping of the methionine responsive genes in amino acid and nucleotide metabolism onto their respective pathways. The schematic shows the methionine-responsive genes in various amino acid and nucleotide biosynthesis pathways, along with their fold-changes in gene expression. The requirement of PPP metabolites, NADPH, PLP or glutamate/glutamine for the individual steps is mapped on to the schematic. The arrows marked red are the steps induced in the presence of methionine. Note that all these regulated steps use PPP intermediates, NADPH, PLP and/or glutamine/glutamate.

B) A bird's eye-view of the amino acid biosynthesis steps regulated by methionine. Each bead (or filled circle) represents a step in the pathway (prepared according to the individual amino acid pathways shown at https://pathway.yeastgenome.org/.) A step is considered expensive (marked red) when it is either the entry or the final or involves ATP utilization or involves reduction. All the rest of the steps are considered inexpensive (marked green). Methionine responsive steps are shown with a yellow fill at the centre of the circle, for the given step. The p-value for methionine dependence of genes encoding the critical, rate-limiting or costly steps in amino acid= $3.8e^{-09}$, and for the other nodes, it is non-significant (Fisher's exact test).

C) A hierarchical organization of the methionine mediated anabolic remodelling. Methionine induces expression of genes in the PPP-GDH-PLP node, which provides precursors for the overall biosynthesis of amino acids and nucleotides.

Figure 4: Gcn4p uniquely regulates the metabolic response due to methionine.

A) Trends of gene expression in RM and methionine supplemented MM in *gcn4Δ* cells. Gene expression levels of transcripts in *gcn4Δ* cells grown in RM or shifted to MM or MM plus methionine or MM plus nonSAAs were compared to WT MM set.

B) Global transcriptional response in the absence of *GCN4*. The heat map shows differentially expressed genes ($\log_2$ 1.5-fold change; $p < 10^{-4}$) between WT and *gcn4Δ* cells in the respective growth conditions.

C) GO analysis of the methionine-responsive genes in *gcn4Δ* cells. A pie chart showing the processes grouped by GO analysis for the up-regulated transcripts between MM plus methionine and MM set in *gcn4Δ* background. Numbers in the bracket indicate the number of genes from the query set/ total number of genes in the reference set for the given GO category.

D) Contribution of *GCN4* to the methionine-response. The expression level of methionine-responsive transcripts in WT set (MM plus methionine versus MM) was compared in the *gcn4Δ* background. Amino acid biosynthesis related genes are marked with blue circles and ribosome biogenesis and function related genes are marked with red circle.

E) Regrouping of the *GCN4*-dependent genes onto metabolic nodes. The schematic shows the *GCN4*-dependent genes (comparison of MM plus methionine set between WT and *gcn4Δ*) in the PPP, amino acid and nucleotide biosynthesis pathways, along with fold-changes in gene expression. The arrows marked blue in the PPP pathway are the steps down-regulated in *gcn4Δ* cells. Key rate-limiting steps in the pathway are marked by asterisk.

Figure 5: Methionine stimulates key transamination and reductive biosynthetic processes.

A) Snz1p, Gnd2p and Gdh1p amounts in WT or *gcn4Δ* cells. WT and *gcn4Δ* cells expressing FLAG-tagged Snz1p or Gnd2p or Gdh1p were shifted from RM to MM or MM plus methionine and amounts of these proteins were detected by Western blotting. A representative blot is shown in each case.

B) NADP-dependent glutamate dehydrogenase activity and methionine availability. Crude extracts of WT cells grown in RM and shifted to MM or MM plus methionine were analysed for intracellular biosynthetic NADP-glutamate dehydrogenase activity.

C) Relative nucleotide amounts in the presence of methionine in WT or *gcn4Δ* cells. WT and *gcn4Δ* cells grown in RM were shifted to MM (4h) with and without methionine, and the relative amounts of AMP and GMP from metabolite extracts of the respective samples were measured by LC-MS/MS.

In all panels data indicate mean±SD. $^{*}p < 0.05$, $^{**}p < 0.01$, $^{***}p < 0.001$.

Figure 6: Methionine stimulates key transamination and reductive biosynthetic processes in amino acid biosynthesis

A) A schematic showing the experimental design of ^{15}N pulse-labelling experiment. Cells were shifted to MM with and without methionine, maintained for 3h, and ^{15}N-ammonium sulfate was pulsed into the medium, and the indicated, labelled metabolites were measured. Also see Table S2.

B) Methionine increases nitrogen assimilation in amino acids. Label incorporation in newly synthesized amino acids in WT and *gcn4Δ* cells was measured, as shown in the panel A. For all the labelled moieties, fractional abundance of the label was calculated. Also see Table S2.

In all panels data indicate mean±SD. $^{*}p < 0.05$, $^{**}p < 0.01$.

Figure 7: Methionine increases nucleotide biosynthesis in a Gcn4p dependent manner.

A) A schematic showing carbon and nitrogen inputs in nucleotide biosynthesis, and their coupling to the PPP/NADPH metabolism.

741 B) Methionine increases nitrogen assimilation in nucleotides. The WT and *gcn4Δ* cells
742 treated and pulse-labelled with ^{15}N ammonium sulfate as illustrated in the top panel. For all
743 the labelled moieties, fractional increase of the incorporated label was calculated, to measure
744 newly synthesized AMP and GMP. (also see Figure S8 for CMP and UMP).

745 C) Methionine enhances carbon flux into AMP biosynthesis. An experimental set-up similar
746 to the Panel B was employed, using ^{13}C-lactate for carbon labelling. Label incorporation into
747 nucleotides (from +1 to +5) was accounted for calculations. (note: GMP could not be
748 estimated because of MS/MS signal interference from unknown compounds in the metabolite
749 extract).
750
751 E) A model illustrating how methionine triggers cell proliferation. Methionine activates the
752 *GCN4*-mediated ISR, promoting the synthesis of PPP metabolites, PLP, NADPH and
753 glutamate (up-regulated genes in the pathways are shown in blue), which directly feed into
754 nitrogen metabolism. As a result, methionine activates biosynthesis of amino acids and
755 nucleotides, allowing the cells to grow in amino acid limiting medium.

756 In all panels data indicate mean±SD. ns: non-significant difference, $^{**}p < 0.01$, $^{***}p < 0.001$.

757

758 **References:**

759 Alam MT, Zelezniak A, Mülleder M, Shliaha P, Schwarz R, Capuano F, Vowinckel J,
760 Radmanesfahar E, Krüger A, Calvani E, Michel S, Börno S, Christen S, Patil KR,
761 Timmermann B, Lilley KS, Ralser M. 2016. The metabolic background is a global
762 player in *Saccharomyces* gene expression epistasis. *Nat Microbiol* **1**:15030.
763 doi:10.1038/nmicrobiol.2015.30.

764 Barton MD, Delneri D, Oliver SG, Rattray M, Bergman CM. 2010. Evolutionary systems
765 biology of amino acid biosynthetic cost in yeast. *PLOS ONE* **5**: e11935.
766 doi:10.1371/journal.pone.0011935

767 Bi M, Naczki C, Koritzinsky M, Fels D, Blais J, Hu N, Harding H, Novoa I, Varia M,
768 Raleigh J, Scheuner D, Kaufman RJ, Bell J, Ron D, Wouters BG, Koumenis C. 2005.
769 ER stress-regulated translation increases tolerance to extreme hypoxia and promotes
770 tumor growth. *EMBO J* **24**:3470-81. doi:10.1038/sj.emboj.7600777.

771 Boer VM, Amini S, Botstein D. 2008. Influence of genotype and nutrition on survival and
772 metabolism of starving yeast. *Proc Natl Acad Sci U S A* **105**:6930-5.
773 doi:10.1073/pnas.0802601105.

774 Boer VM, Crutchfield CA, Bradley PH, Botstein D, Rabinowitz JD. 2010. Growth-limiting
775 intracellular metabolites in yeast growing under diverse nutrient limitations. *Mol Biol*
776 *Cell* **21**:198-211. doi:10.1091/mbc.E09-07-0597.

777 Brachmann CB, Davies A, Cost GJ, Caputo E, Li J, Hieter P, Boeke JD. 1998. Designer
778 deletion strains derived from *Saccharomyces cerevisiae* S288C: A useful set of strains
779 and plasmids for PCR-mediated gene disruption and other applications. *Yeast* **14**:115-32.
780 doi:10.1002/(SICI)1097-0061(19980130)14:2<115::AID-YEA204>3.0.CO;2-2.

781 Brauer MJ, Huttenhower C, Airoldi EM, Rosenstein R, Matese JC, Gresham D, Boer VM,
782 Troyanskaya OG, Botstein D. 2008. Coordination of growth rate, cell cycle, stress

783 response, and metabolic activity in yeast. *Mol Biol Cell* **19**:352-67.
784 doi:10.1091/mbc.E07-08-0779.
785 Breillout F, Antoine E, Poupon MF. 1990. Methionine dependency of malignant tumors: A
786 possible approach for therapy. *J Natl Cancer Inst* **82**:1628-32.
787 doi:10.1093/jnci/82.20.1628.
788 Broach JR. 2012. Nutritional control of growth and development in yeast. *Genetics* **192**:73-
789 105. doi:10.1534/genetics.111.135731.
790 Cai L, Sutter BM, Li B, Tu BP. 2011. Acetyl-CoA induces cell growth and proliferation by
791 promoting the acetylation of histones at growth genes. *Mol Cell* **42**:426-37.
792 doi:10.1016/j.molcel.2011.05.004.
793 Cairns RA, Harris IS, Mak TW. 2011. Regulation of cancer cell metabolism. *Nat Rev Cancer*
794 **11**:85-95. doi:10.1038/nrc2981.
795 Campbell K, Vowinckel J, Keller MA, Ralser M. 2016. Methionine metabolism alters
796 oxidative stress resistance *via* the pentose phosphate pathway. *Antioxid Redox Signal*
797 **24**:543-7. doi:10.1089/ars.2015.6516.
798 Carmona-Saez P, Chagoyen M, Tirado F, Carazo JM, Pascual-Montano A. 2007.
799 GENECODIS: A web-based tool for finding significant concurrent annotations in gene
800 lists. *Genome Biol* **8**:R3.
801 Caspi R, Altman T, Billington R, Dreher K, Foerster H, Fulcher CA, Holland TA, Keseler
802 IM, Kothari A, Kubo A, Krummenacker M, Latendresse M, Mueller LA, Ong Q, Paley
803 S, Subhraveti P, Weaver DS, Weerasinghe D, Zhang P, Karp PD. 2014. The MetaCyc
804 database of metabolic pathways and enzymes and the BioCyc collection of
805 pathway/genome databases. *Nucleic Acids Res* **42**:D459-71. doi:10.1093/nar/gkt1103.
806 Cavuoto P, Fenech MF. 2012. A review of methionine dependency and the role of
807 methionine restriction in cancer growth control and life-span extension. *Cancer Treat*

808 *Rev* **38**:726-36. doi:10.1016/j.ctrv.2012.01.004.
809 Cellarier E, Durando X, Vasson MP, Farges MC, Demiden A, Maurizis JC, Madelmont JC,
810 Chollet P. 2003. Methionine dependency and cancer treatment. *Cancer Treat Rev*
811 **29**:489-99. doi:10.1016/S0305-7372(03)00118-X.
812 Clarke CJ, Berg TJ, Birch J, Ennis D, Mitchell L, Cloix C, Campbell A, Sumpton D, Nixon
813 C, Campbell K, Bridgeman VL, Vermeulen PB, Foo S, Kostaras E, Jones JL, Haywood
814 L, Pulleine E, Yin H, Strathdee D, Sansom O, Blyth K, McNeish I, Zanivan S, Reynolds
815 AR, Norman JC. 2016. The initiator methionine tRNA drives secretion of type II
816 collagen from stromal fibroblasts to promote tumor growth and angiogenesis. *Curr Biol*
817 **26**:755-65. doi:10.1016/j.cub.2016.01.045.
818 Collart MA, Oliviero S. 2001. Preparation of yeast RNA. In *Curr Protoc Mol Biol*. Hoboken,
819 NJ, USA: John Wiley & Sons, Inc. doi:10.1002/0471142727.mb1312s23.
820 Comerford SA, Huang Z, Du X, Wang Y, Cai L, Witkiewicz AK, Walters H, Tantawy MN,
821 Fu A, Manning HC, Horton JD, Hammer RE, McKnight SL, Tu BP. 2014. Acetate
822 dependence of tumors. *Cell* **159**:1591-1602. doi:10.1016/j.cell.2014.11.020.
823 Corbacho I, Teixidó F, Velázquez R, Hernández LM, Olivero I. 2011. Standard YPD, even
824 supplemented with extra nutrients, does not always compensate growth defects of
825 *Saccharomyces cerevisiae* auxotrophic strains. *Antonie Van Leeuwenhoek* **99**:591-600.
826 doi:10.1007/s10482-010-9530-5.
827 DeBerardinis RJ, Sayed N, Ditsworth D, Thompson CB. 2008. Brick by brick: Metabolism
828 and tumor cell growth. *Curr Opin Genet Dev* **18**:54-61. doi:10.1016/j.gde.2008.02.003.
829 Dechant R, Peter M. 2008. Nutrient signals driving cell growth. *Curr Opin Cell Biol* **20**:678-
830 87. doi:10.1016/j.ceb.2008.09.009.
831 Doherty D. 1970. [119] L-Glutamate dehydrogenases (yeast). In , 850-56. doi:10.1016/0076-
832 6879(71)17294-1.

833 Dong YX, Sueda S, Nikawa JI, Kondo H. 2004. Characterization of the products of the genes
834 *SNO1* and *SNZ1* involved in pyridoxine synthesis in *Saccharomyces cerevisiae*. *Eur J*
835 *Biochem* **271**: 745-52. doi:10.1111/j.1432-1033.2003.03973.x.
836 Dwight SS, Harris MA, Dolinski K, Ball CA, Binkley G, Christie KR, Fisk DG, Issel-Tarver
837 L, Schroeder M, Sherlock G, Sethuraman A, Weng S, Botstein D, Cherry JM. 2002.
838 Saccharomyces Genome Database (SGD) provides secondary gene annotation using the
839 Gene Ontology (GO). *Nucleic Acids Res* **30**:69-72. doi:10.1093/nar/30.1.69.
840 Eliot AC, Kirsch JF. 2004. Pyridoxal phosphate enzymes: Mechanistic, structural, and
841 evolutionary considerations. *Annu Rev Biochem* **73**:383-415.
842 doi:10.1146/annurev.biochem.73.011303.074021.
843 Faubert B, Li KY, Cai L, Hensley CT, Kim J, Zacharias LG, Yang C, Do QN, Doucette S,
844 Burguete D, Li H, Huet G, Yuan Q, Wigal T, Butt Y, Ni M, Torrealba J, Oliver D,
845 Lenkinski RE, Malloy CR, Wachsmann JW, Young JD, Kernstine K, DeBerardinis RJ.
846 2017. Lactate metabolism in human lung tumors. *Cell* **171**:358-371.e9.
847 doi:10.1016/j.cell.2017.09.019.
848 Fauchon M, Lagniel G, Aude JC, Lombardia L, Soularue P, Petat C, Marguerie G, Sentenac
849 A, Werner M, Labarre J. 2002. Sulfur sparing in the yeast proteome in response to sulfur
850 demand. *Mol Cell* **9**:713-23. doi:10.1016/S1097-2765(02)00500-2.
851 Gerashchenko MV, Gladyshev VN. 2014. Translation inhibitors cause abnormalities in
852 ribosome profiling experiments. *Nucleic Acids Res* **42**:e134. doi:10.1093/nar/gku671.
853 Gray JV, Petsko GA, Johnston GC, Ringe D, Singer RA, Werner-Washburne M. 2004.
854 "Sleeping Beauty": Quiescence in *Saccharomyces cerevisiae*. *Microbiol Mol Biol Rev*
855 **68**:187-206. doi:10.1128/MMBR.68.2.187-206.2004.
856 Guo HY, Herrera H, Groce A, Hoffman RM. 1993. Expression of the biochemical defect of
857 methionine dependence in fresh patient tumors in primary histoculture. *Cancer Res*

858 **53**:2479-83. PMID:8495409.

859 Halpern BC, Clark BR, Hardy DN, Halpern RM, Smith RA. 1974. The effect of replacement
860 of methionine by homocystine on survival of malignant and normal adult mammalian
861 cells in culture. *Proc Natl Acad Sci U S A* **71**:1133-36. doi:10.1073/pnas.71.4.1133.

862 Hinnebusch AG. 2005. Translational regulation of *GCN4* and the general amino acid control
863 of yeast. *Annu Rev Microbiol* **59**:407-50. doi:10.1146/annurev.micro.59.031805.133833.

864 Hu X, Chao M, Wu H. 2017. Central role of lactate and proton in cancer cell resistance to
865 glucose deprivation and its clinical translation. *Signal Transduct Target Ther* **2**:e16047.
866 doi: 10.1038/sigtrans.2016.47.

867 Jorgensen P, Tyers M. 2004. How cells coordinate growth and division. *Curr Biol* **14**:R1014-
868 27. doi:10.1016/j.cub.2004.11.027.

869 Kaleta C, Schäuble S, Rinas U, Schuster S. 2013. Metabolic costs of amino acid and protein
870 production in *Escherichia coli*. *Biotechnol J* **8**:1105-14. doi:10.1002/biot.201200267.

871 Kennedy KM, Scarbrough PM, Ribeiro A, Richardson R, Yuan H, Sonveaux P, Landon CD,
872 Chi JT, Pizzo S, Schroeder T, Dewhirst MW. 2013. Catabolism of exogenous lactate
873 reveals it as a legitimate metabolic substrate in breast cancer. *PLOS ONE* **8**: e75154.
874 doi:10.1371/journal.pone.0075154.

875 Klosinska MM, Crutchfield CA, Bradley PH, Rabinowitz JD, Broach JR. 2011. Yeast cells
876 can access distinct quiescent states. *Genes Dev* **25**:336-49. doi:10.1101/gad.2011311.

877 Kokkinakis DM, Hoffman RM, Frenkel EP, Wick JB, Han Q, Xu M, Tan Y, Schold SC.
878 2001. Synergy between methionine stress and chemotherapy in the treatment of brain
879 tumor xenografts in athymic mice. *Cancer Res* **61**:4017-23. PMID:11358820.

880 Laxman S, Sutter BM, Shi L, Tu BP. 2014. Npr2 inhibits TORC1 to prevent inappropriate
881 utilization of glutamine for biosynthesis of nitrogen-containing metabolites. *Sci Signal*
882 **7**:ra120. doi:10.1126/scisignal.2005948.

883 Laxman S, Sutter BM, Wu X, Kumar S, Guo X, Trudgian DC, Mirzaei H, Tu BP. 2013.
884 Sulfur amino acids regulate translational capacity and metabolic homeostasis through
885 modulation of tRNA thiolation. *Cell* **154**:416-29. doi:10.1016/j.cell.2013.06.043.
886 Laxman S, Tu BP. 2010. Systems approaches for the study of metabolic cycles in yeast. *Curr*
887 *Opin Genet Dev* **20**:599-604. doi:10.1016/j.gde.2010.09.008.
888 Lee BC, Kaya A, Gladyshev VN. 2016. Methionine restriction and life-span control. *Ann N Y*
889 *Acad Sci* **1363**:116-24. doi:10.1111/nyas.12973.
890 Lee BC, Kaya A, Ma S, Kim G, Gerashchenko MV, Yim SH, Hu Z, Harshman LG,
891 Gladyshev VN. 2014. Methionine restriction extends lifespan of *Drosophila*
892 *melanogaster* under conditions of low amino-acid status. *Nat Commun* **5**:3592.
893 doi:10.1038/ncomms4592.
894 Li H, Durbin R. 2009. Fast and accurate short read alignment with Burrows-Wheeler
895 transform. *Bioinformatics* **25**:1754-60. doi:10.1093/bioinformatics/btp324.
896 Ljungdahl PO, Daignan-Fornier B. 2012. Regulation of amino acid, nucleotide, and
897 phosphate metabolism in *Saccharomyces cerevisiae*. *Genetics* **190**:885-929.
898 doi:10.1534/genetics.111.133306.
899 Lu S, Epner DE. 2000. Molecular mechanisms of cell cycle block by methionine restriction
900 in human prostate cancer cells. *Nutr Cancer* **38**:123-30.
901 doi:10.1207/S15327914NC381_17.
902 Mampel J, Schröder H, Haefner S, Sauer U. 2005. Single-gene knockout of a novel
903 regulatory element confers ethionine resistance and elevates methionine production in
904 *Corynebacterium glutamicum*. *Appl Microbiol Biotechnol* **68**:228-36.
905 doi:10.1007/s00253-005-1893-6.
906 Mariño, G, Pietrocola F, Eisenberg T, Kong Y, Malik SA, Andryushkova A, Schroeder S,
907 Pendl T, Harger A, Niso-Santano M, Zamzami N, Scoazec M, Durand S, Enot DP,

908 Fernández ÁF, Martins I, Kepp O, Senovilla L, Bauvy C, Morselli E, Vacchelli E,
909 Bennetzen M, Magnes C, Sinner F, Pieber T, López-Otín C, Maiuri MC, Codogno P,
910 Andersen JS, Hill JA, Madeo F, Kroemer G. 2014. Regulation of autophagy by cytosolic
911 acetyl-coenzyme A. *Mol Cell* **53**:710-25. doi:10.1016/j.molcel.2014.01.016.
912 Natarajan K, Meyer MR, Jackson BM, Slade D, Roberts C, Hinnebusch AG, Marton MJ.
913 2001. Transcriptional profiling shows that Gcn4p is a master regulator of gene
914 expression during amino acid starvation in yeast. *Mol Cell Biol* **21**:4347-68.
915 doi:10.1128/MCB.21.13.4347-4368.2001.
916 Nelson DL, Cox MM. 2017. Lehninger Principles of Biochemistry (7th ed.). New York:W. H.
917 Freeman. p. 533-74.
918 Nogales-Cadenas R, Carmona-Saez P, Vazquez M, Vicente C, Yang X, Tirado F, Carazo JM,
919 Pascual-Montano A. 2009. GeneCodis: interpreting gene lists through enrichment
920 analysis and integration of diverse biological information. *Nucleic Acids Res* **37**:W317-
921 22. doi:10.1093/nar/gkp416.
922 Palam LR, Gore J, Craven KE, Wilson JL, Korc M. 2015. Integrated stress response is
923 critical for gemcitabine resistance in pancreatic ductal adenocarcinoma. *Cell Death Dis*
924 **6**:e1913. doi:10.1038/cddis.2015.264.
925 Patra KC, Hay N. 2014. The pentose phosphate pathway and cancer. *Trends Biochem Sci*
926 **39**:347-54. doi:10.1016/j.tibs.2014.06.005.
927 Pietrocola F, Galluzzi L, Bravo-San Pedro JM, Madeo F, Kroemer G. 2015. Acetyl coenzyme
928 A: A central metabolite and second messenger. *Cell Metab* **21**:805-21.
929 doi:10.1016/j.cmet.2015.05.014.
930 Poirson-Bichat F, Gonçalves RA, Miccoli L, Dutrillaux B, Poupon MF. 2000. Methionine
931 depletion enhances the antitumoral efficacy of cytotoxic agents in drug-resistant human
932 tumor xenografts. *Clin Cancer Res* **6**:643-53. PMID:10690550.

933 Pronk JT. 2002. Auxotrophic yeast strains in fundamental and applied research. *Appl Environ*
934 *Microbiol* **68**:2095-2100. doi:10.1128/AEM.68.5.2095-2100.2002.
935 Robinson MD, McCarthy DJ, Smyth GK. 2010. edgeR: A bioconductor package for
936 differential expression analysis of digital gene expression data. *Bioinformatics* **26**:139-
937 40. doi:10.1093/bioinformatics/btp616.
938 Sherman F. 1991. Getting started with yeast. *Methods Enzymol* **194**:3-21. doi:10.1016/0076-
939 6879(91)94004-V.
940 Shi L, Tu BP. 2013. Acetyl-CoA induces transcription of the key G1 cyclin *CLN3* to promote
941 entry into the cell division cycle in *Saccharomyces cerevisiae*. *Proc Natl Acad Sci U S A*
942 **110**:7318-23. doi:10.1073/pnas.1302490110.
943 Slavov N, Botstein D. 2011. Coupling among growth rate response, metabolic cycle, and cell
944 division cycle in yeast. *Mol Biol Cell* **22**:1997-2009. doi:10.1091/mbc.E11-02-0132.
945 Slavov N, Botstein D. 2013. Decoupling nutrient signaling from growth rate causes aerobic
946 glycolysis and deregulation of cell size and gene expression. *Mol Biol Cell* **24**:157-68.
947 doi:10.1091/mbc.E12-09-0670.
948 Srinivasan R, Chandraprakash D, Krishnamurthi R, Singh P, Scolari VF, Krishna S,
949 Seshasayee AS. 2013. Genomic analysis reveals epistatic silencing of "expensive" genes
950 in *Escherichia coli* K-12. *Mol Biosyst* **9**:2021-33. doi:10.1039/c3mb70035f.
951 Stern PH, Hoffman RM. 1986. Enhanced *in vitro* selective toxicity of chemotherapeutic
952 agents for human cancer cells based on a metabolic defect. *J Natl Cancer Inst* **76**:629-
953 39. doi:10.1093/jnci/76.4.629.
954 Sugimura T, Birnbaum SM, Winitz M, Greenstein JP. 1959. Quantitative nutritional studies
955 with water-soluble, chemically defined diets. VIII. The forced feeding of diets each
956 lacking in one essential amino acid. *Arch Biochem Biophys* **81**:448-55.
957 doi:10.1016/0003-9861(59)90225-5.

958 Sutter BM, Wu X, Laxman S, Tu BP. 2013. Methionine inhibits autophagy and promotes
959 growth by inducing the SAM-responsive methylation of PP2A. *Cell* **154**:403-15.
960 doi:10.1016/j.cell.2013.06.041.
961 Tabas-Madrid D, Nogales-Cadenas R, Pascual-Montano A. 2012. GeneCodis3: a non-
962 redundant and modular enrichment analysis tool for functional genomics. *Nucleic Acids*
963 *Res* **40**:W478-83. doi:10.1093/nar/gks402.
964 Thomas D, Cherest H, Surdin-Kerjan Y. 1991. Identification of the structural gene for
965 glucose-6-phosphate dehydrogenase in yeast. Inactivation leads to a nutritional
966 requirement for organic sulfur. *EMBO J* **10**:547-53. PMID:2001672.
967 Thomas D, Surdin-Kerjan Y. 1997. Metabolism of sulfur amino acids in *Saccharomyces*
968 *cerevisiae*. *Microbiol Mol Biol Rev* **61**:503-32. PMID:9409150.
969 Tong X, Zhao F, Thompson CB. 2009. The molecular determinants of *de novo* nucleotide
970 biosynthesis in cancer cells. *Curr Opin Genet Dev* **19**:32-37.
971 doi:10.1016/j.gde.2009.01.002.
972 Troen AM, French EE, Roberts JF, Selhub J, Ordovas JM, Parnell LD, Lai CQ. 2007.
973 Lifespan modification by glucose and methionine in *Drosophila melanogaster* fed a
974 chemically defined diet. *Age (Dordr)* **29**:29-39. doi:10.1007/s11357-006-9018-4.
975 Tu BP, Kudlicki A, Rowicka M, McKnight SL. 2005. Logic of the yeast metabolic cycle:
976 Temporal compartmentalization of cellular processes. *Science* **310**:1152-58.
977 doi:10.1126/science.1120499.
978 Tu BP, Mohler RE, Liu JC, Dombek KM, Young ET, Synovec RE, McKnight SL. 2007.
979 Cyclic changes in metabolic state during the life of a yeast cell. *Proc Natl Acad Sci U S*
980 *A* **104**:16886-91. doi:10.1073/pnas.0708365104.
981 Unger MW, Hartwell LH. 1976. Control of cell division in *Saccharomyces cerevisiae* by
982 methionyl-tRNA. *Proc Natl Acad Sci U S A* **73**:1664-68. doi:10.1073/pnas.73.5.1664.

983 van Dijken JP, Bauer J, Brambilla L, Duboc P, Francois JM, Gancedo C, Giuseppin ML,
984 Heijnen JJ, Hoare M, Lange HC, Madden EA, Niederberger P, Nielsen J, Parrou JL,
985 Petit T, Porro D, Reuss M, van Riel N, Rizzi M, Steensma HY, Verrips CT, Vindeløv J,
986 Pronk JT. 2000. An interlaboratory comparison of physiological and genetic properties
987 of four *Saccharomyces cerevisiae* strains. *Enzyme Microb Technol* **26**:706-14.
988 doi:10.1016/S0141-0229(00)00162-9.
989 Vander Heiden MG, Cantley LC, Thompson CB. 2009. Understanding the Warburg effect:
990 The metabolic requirements of cell proliferation. *Science* **324**:1029-33.
991 doi:10.1126/science.1160809.
992 Vattem KM, Wek RC. 2004. Reinitiation involving upstream ORFs regulates *ATF4* mRNA
993 translation in mammalian cells. *Proc Natl Acad Sci U S A* **101**:11269-74.
994 doi:10.1073/pnas.0400541101.
995 Warburg O. 1956. On the origin of cancer cells. *Science* **123**:309-14.
996 doi:10.1126/science.123.3191.309.
997 Warner JR, Vilardell J, Sohn JH. 2001. Economics of ribosome biosynthesis. *Cold Spring*
998 *Harb Symp Quant Biol* **66**:567-74. doi:10.1101/sqb.2001.66.567.
999 Warner JR. 1999. The economics of ribosome biosynthesis in yeast. *Trends Biochem Sci*
1000 **24**:437-40. doi:10.1016/S0968-0004(99)01460-7.
1001 Wu X, Tu BP. 2011. Selective regulation of autophagy by the Iml1-Npr2-Npr3 complex in
1002 the absence of nitrogen starvation. *Mol Biol Cell* **22**:4124-33. doi:10.1091/mbc.E11-06-
1003 0525.
1004 Xu YF, Létisse F, Absalan F, Lu W, Kuznetsova E, Brown G, Caudy AA, Yakunin AF,
1005 Broach JR, Rabinowitz JD. 2013. Nucleotide degradation and ribose salvage in yeast.
1006 *Mol Syst Biol* **9**:665. doi:10.1038/msb.2013.21.
1007 Ye J, Kumanova M, Hart LS, Sloane K, Zhang H, De Panis DN, Bobrovnikova-Marjon E,

1008 Diehl JA, Ron D, Koumenis C. 2010. The *GCN2-ATF4* pathway is critical for tumour
1009 cell survival and proliferation in response to nutrient deprivation. *EMBO J* **29**:2082-96.
1010 doi:10.1038/emboj.2010.81.

Figure 1

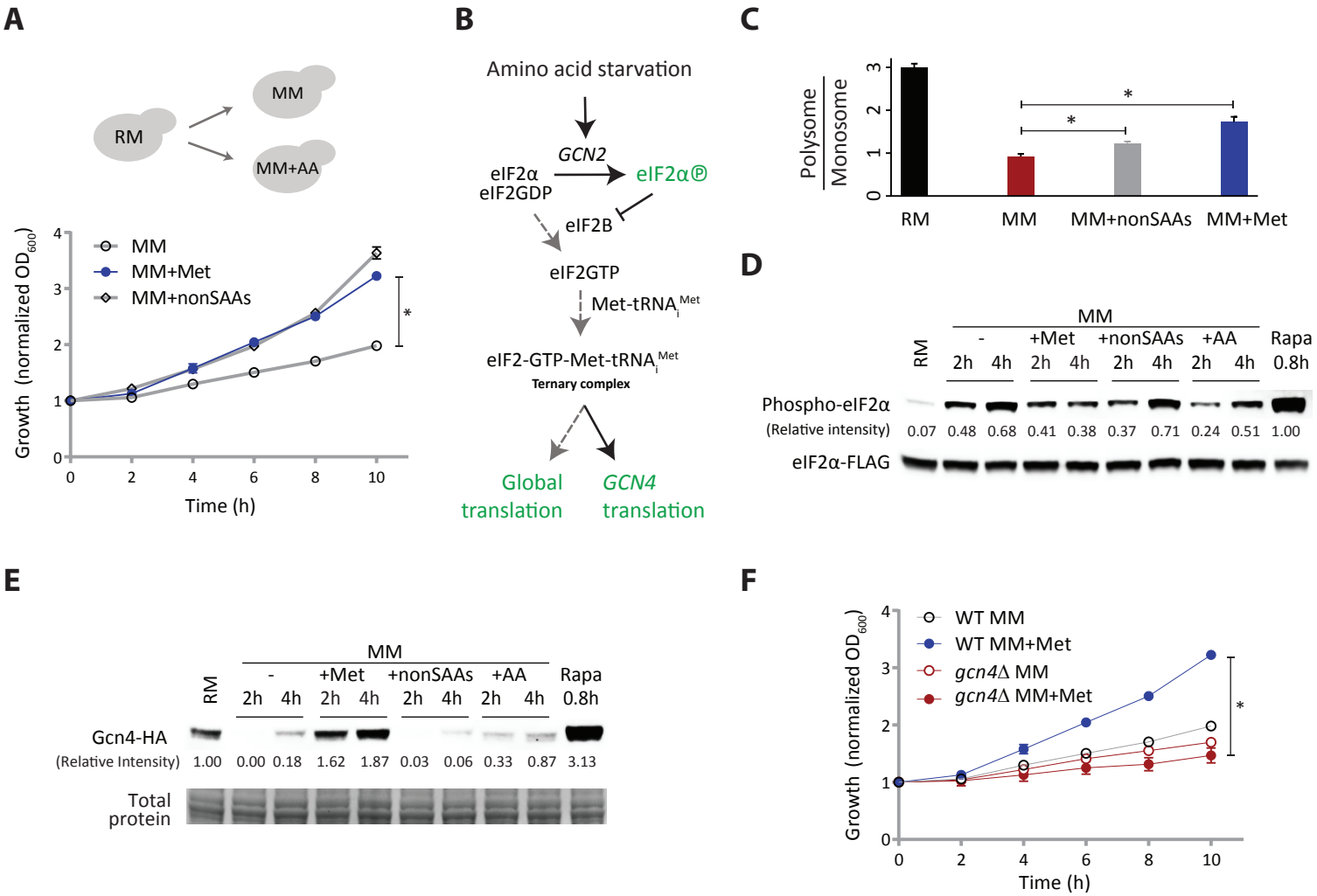
A
RM
MM
MM+AA
MM
MM+Met
MM+nonSAAs
Growth (normalized OD600)
Time (h)
*
B
Amino acid starvation
GCN2
eIF2α
eIF2GDP
eIF2α℗
eIF2B
eIF2GTP
Met-tRNAi Met
eIF2-GTP-Met-tRNAi Met
Ternary complex
Global translation
GCN4 translation
C
Polysome
Monosome
RM
MM
MM+nonSAAs
MM+Met
*
*
D
RM
MM
-
+Met
+nonSAAs
+AA
Rapa
2h 4h 2h 4h 2h 4h 2h 4h
0.8h
Phospho-eIF2α
(Relative intensity) 0.07 0.48 0.68 0.41 0.38 0.37 0.71 0.24 0.51 1.00
eIF2α-FLAG
E
RM
MM
-
+Met
+nonSAAs
+AA
Rapa
2h 4h 2h 4h 2h 4h 2h 4h
0.8h
Gcn4-HA
(Relative Intensity) 1.00 0.00 0.18 1.62 1.87 0.03 0.06 0.33 0.87 3.13
Total protein
F
WT MM
WT MM+Met
gcn4Δ MM
gcn4Δ MM+Met
Growth (normalized OD600)
Time (h)
*

Figure 2

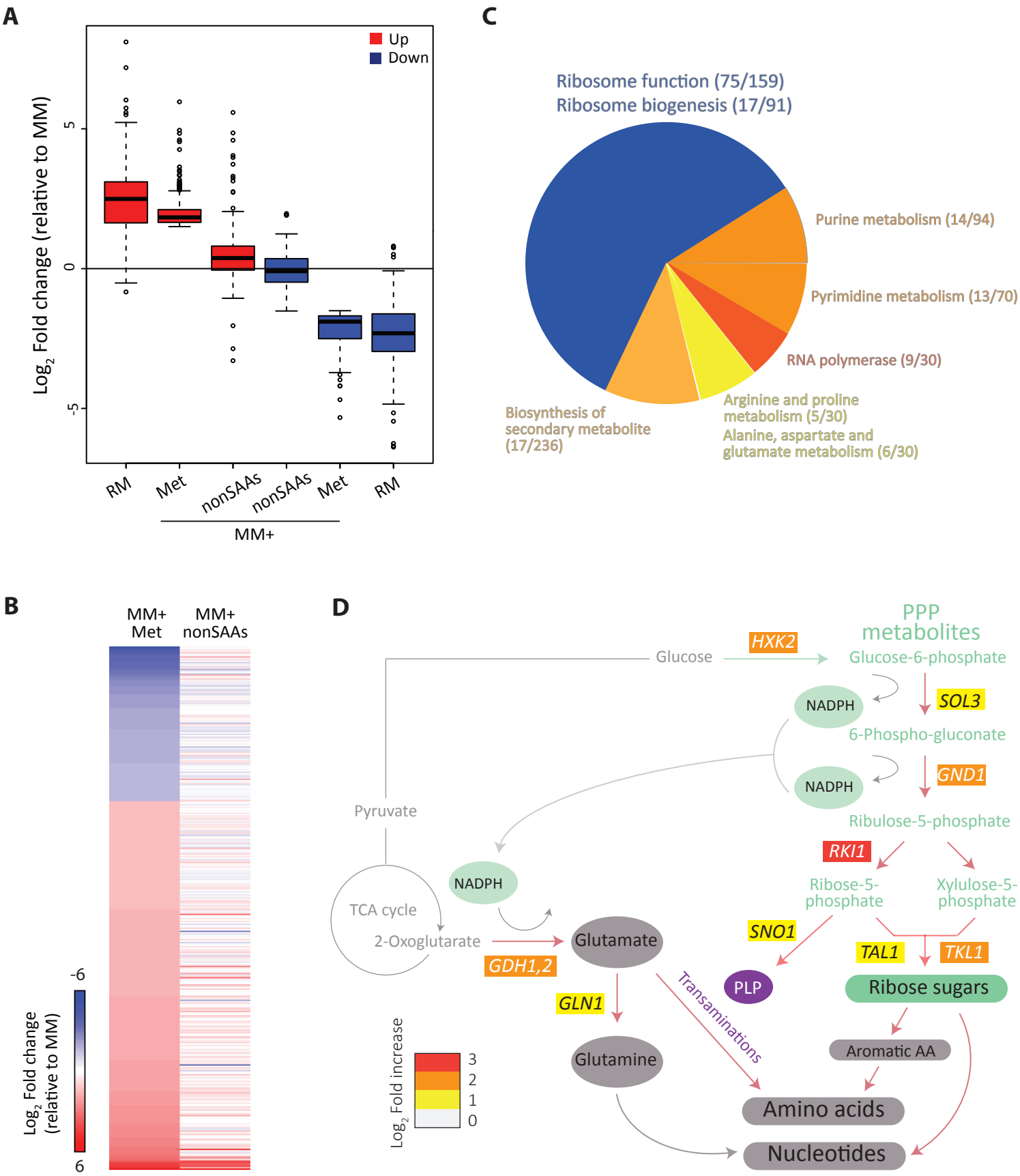
A
Up
Down
Log2 Fold change (relative to MM)
5
0
-5
RM
Met
nonSAAs
nonSAAs
Met
RM
MM+
C
Ribosome function (75/159)
Ribosome biogenesis (17/91)
Purine metabolism (14/94)
Pyrimidine metabolism (13/70)
RNA polymerase (9/30)
Arginine and proline metabolism (5/30)
Alanine, aspartate and glutamate metabolism (6/30)
Biosynthesis of secondary metabolite (17/236)
B
MM+ Met
MM+ nonSAAs
Log2 Fold change (relative to MM)
-6
6
D
Glucose
HXK2
PPP metabolites
Glucose-6-phosphate
NADPH
SOL3
6-Phospho-gluconate
NADPH
GND1
Ribulose-5-phosphate
RKI1
Ribose-5-phosphate
Xylulose-5-phosphate
Pyruvate
NADPH
TCA cycle
2-Oxoglutarate
GDH1,2
Glutamate
SNO1
TAL1
TKL1
PLP
Ribose sugars
GLN1
Transaminations
Glutamine
Aromatic AA
Amino acids
Nucleotides
Log2 Fold increase
3
2
1
0

Figure 3

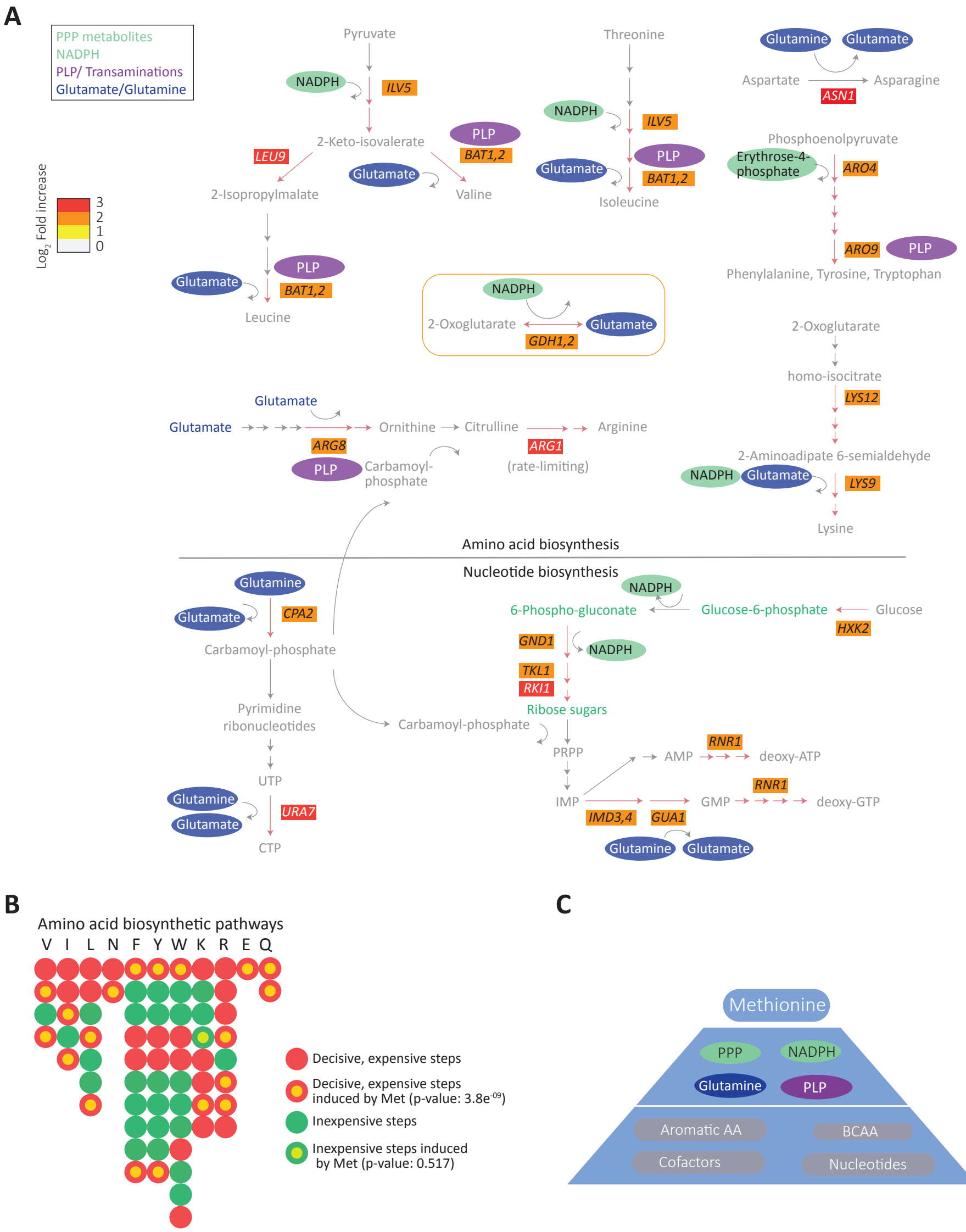
A
PPP metabolites
NADPH
PLP/ Transaminations
Glutamate/Glutamine
Log2 Fold increase
3
2
1
0
Pyruvate
NADPH
ILV5
2-Keto-isovalerate
LEU9
2-Isopropylmalate
PLP
BAT1,2
Glutamate
Valine
Threonine
NADPH
ILV5
PLP
BAT1,2
Glutamate
Isoleucine
Glutamine
Glutamate
Aspartate
ASN1
Asparagine
Phosphoenolpyruvate
Erythrose-4-phosphate
ARO4
ARO9
PLP
Phenylalanine, Tyrosine, Tryptophan
Glutamate
PLP
BAT1,2
Leucine
NADPH
2-Oxoglutarate
Glutamate
GDH1,2
2-Oxoglutarate
homo-isocitrate
LYS12
2-Aminoadipate 6-semialdehyde
NADPH
Glutamate
LYS9
Lysine
Glutamate
Glutamate
ARG8
Ornithine
Citrulline
ARG1
(rate-limiting)
Arginine
PLP
Carbamoyl-phosphate
Amino acid biosynthesis
Nucleotide biosynthesis
Glutamine
Glutamate
CPA2
Carbamoyl-phosphate
Pyrimidine ribonucleotides
UTP
Glutamine
Glutamate
URA7
CTP
NADPH
6-Phospho-gluconate
Glucose-6-phosphate
Glucose
HXK2
GND1
NADPH
TKL1
RKI1
Ribose sugars
Carbamoyl-phosphate
PRPP
AMP
RNR1
deoxy-ATP
IMP
IMD3,4
GUA1
GMP
RNR1
deoxy-GTP
Glutamine
Glutamate

B
Amino acid biosynthetic pathways
V I L N F Y W K R E Q
Decisive, expensive steps
Decisive, expensive steps induced by Met (p-value: 3.8e-09)
Inexpensive steps
Inexpensive steps induced by Met (p-value: 0.517)

C
Methionine
PPP
NADPH
Glutamine
PLP
Aromatic AA
BCAA
Cofactors
Nucleotides

Figure 4

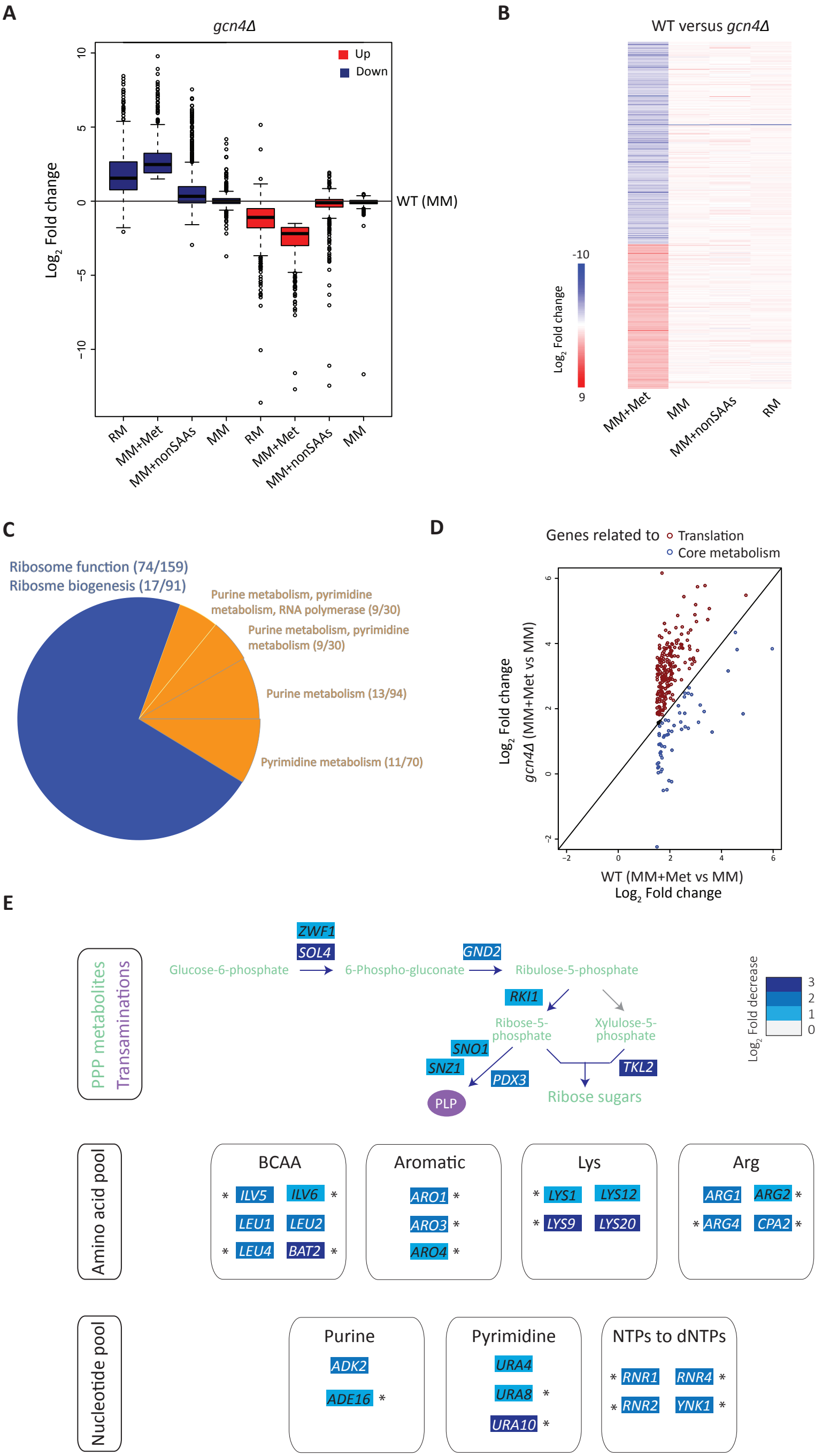
A
gcn4Δ
Up
Down
Log2 Fold change
WT (MM)
RM
MM+Met
MM+nonSAAs
MM
B
WT versus gcn4Δ
Log2 Fold change
-10
9
MM+Met
MM
MM+nonSAAs
RM
C
Ribosome function (74/159)
Ribosme biogenesis (17/91)
Purine metabolism, pyrimidine metabolism, RNA polymerase (9/30)
Purine metabolism, pyrimidine metabolism (9/30)
Purine metabolism (13/94)
Pyrimidine metabolism (11/70)
D
Genes related to
Translation
Core metabolism
Log2 Fold change gcn4Δ (MM+Met vs MM)
WT (MM+Met vs MM) Log2 Fold change
E
PPP metabolites
Transaminations
ZWF1
SOL4
GND2
Glucose-6-phosphate
6-Phospho-gluconate
Ribulose-5-phosphate
RKI1
Ribose-5-phosphate
Xylulose-5-phosphate
SNO1
SNZ1
PDX3
TKL2
PLP
Ribose sugars
Log2 Fold decrease
3
2
1
0
Amino acid pool
BCAA
ILV5
ILV6
LEU1
LEU2
LEU4
BAT2
Aromatic
ARO1
ARO3
ARO4
Lys
LYS1
LYS12
LYS9
LYS20
Arg
ARG1
ARG2
ARG4
CPA2
Nucleotide pool
Purine
ADK2
ADE16
Pyrimidine
URA4
URA8
URA10
NTPs to dNTPs
RNR1
RNR4
RNR2
YNK1

Figure 5

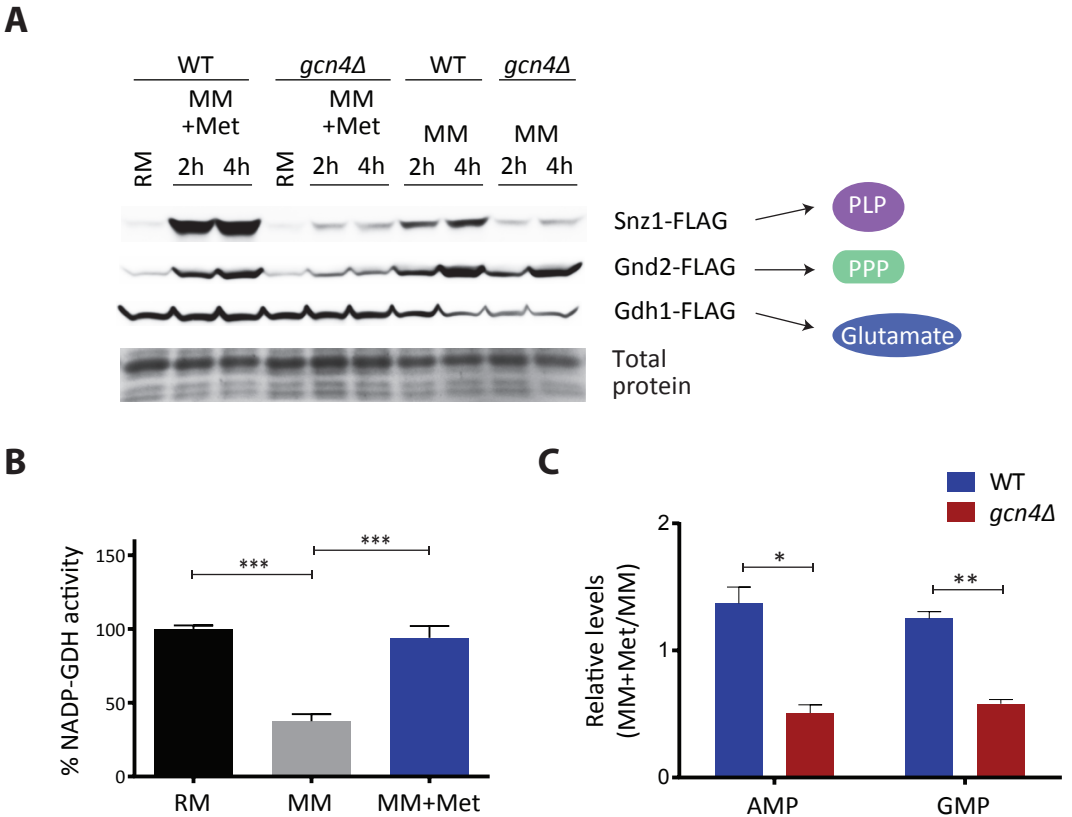
A
WT
gcn4Δ
WT
gcn4Δ
MM +Met
MM +Met
MM
MM
RM
2h 4h
RM
2h 4h
2h 4h
2h 4h
Snz1-FLAG
Gnd2-FLAG
Gdh1-FLAG
Total protein
PLP
PPP
Glutamate
B
% NADP-GDH activity
150
100
50
0
***
***
RM
MM
MM+Met
C
WT
gcn4Δ
Relative levels (MM+Met/MM)
2
1
0
*
**
AMP
GMP

Figure 6

A

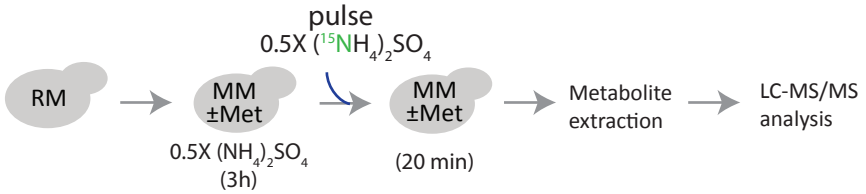
pulse
0.5X ($^{15}NH_4)_2SO_4$
RM
MM ±Met
0.5X $(NH_4)_2SO_4$ (3h)
MM ±Met
(20 min)
Metabolite extraction
LC-MS/MS analysis

B

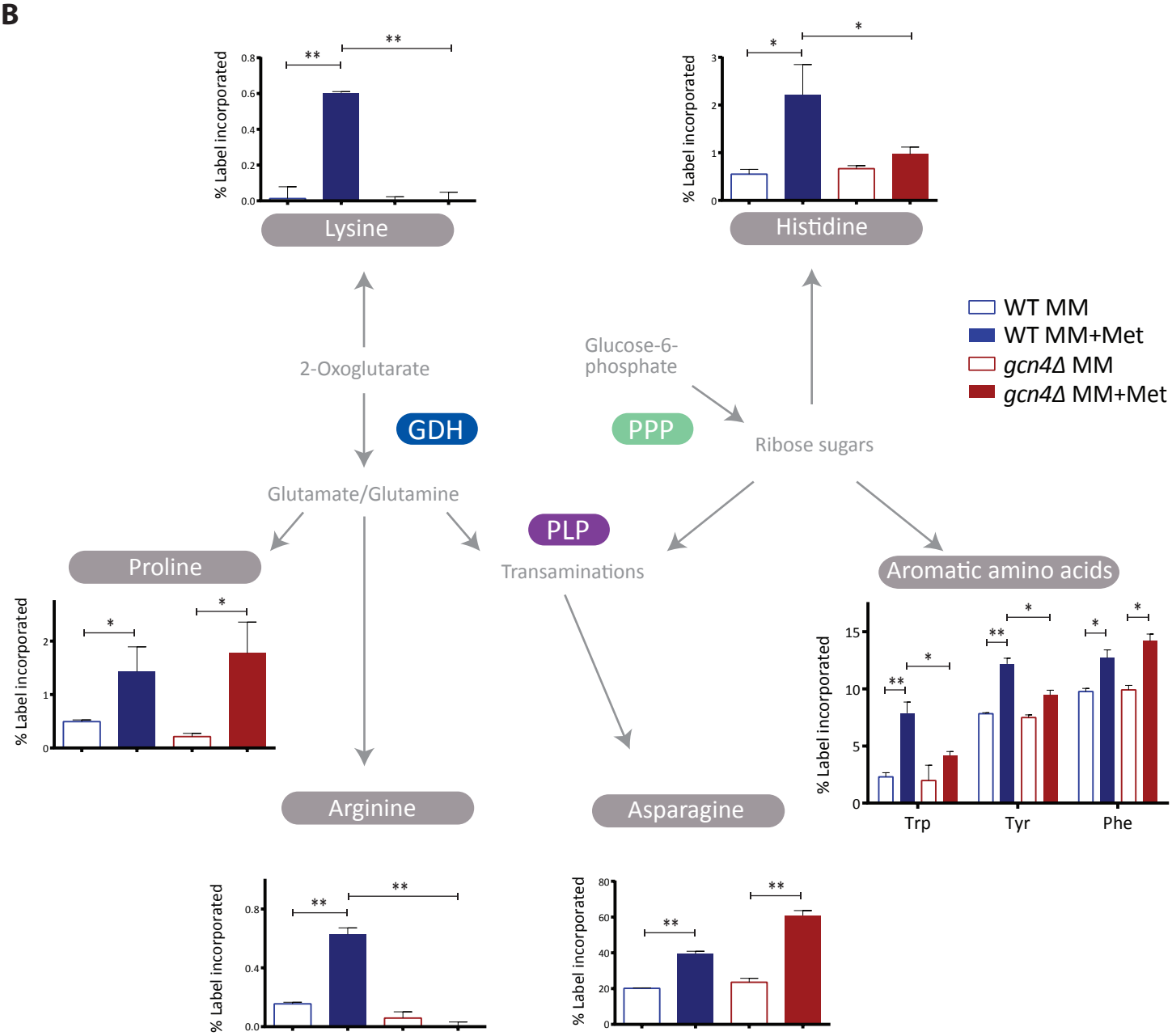
% Label incorporated
Lysine
Histidine
WT MM
WT MM+Met
gcn4Δ MM
gcn4Δ MM+Met
2-Oxoglutarate
Glucose-6-phosphate
GDH
PPP
Ribose sugars
Glutamate/Glutamine
PLP
Transaminations
Proline
Aromatic amino acids
Trp
Tyr
Phe
Arginine
Asparagine

Figure 7

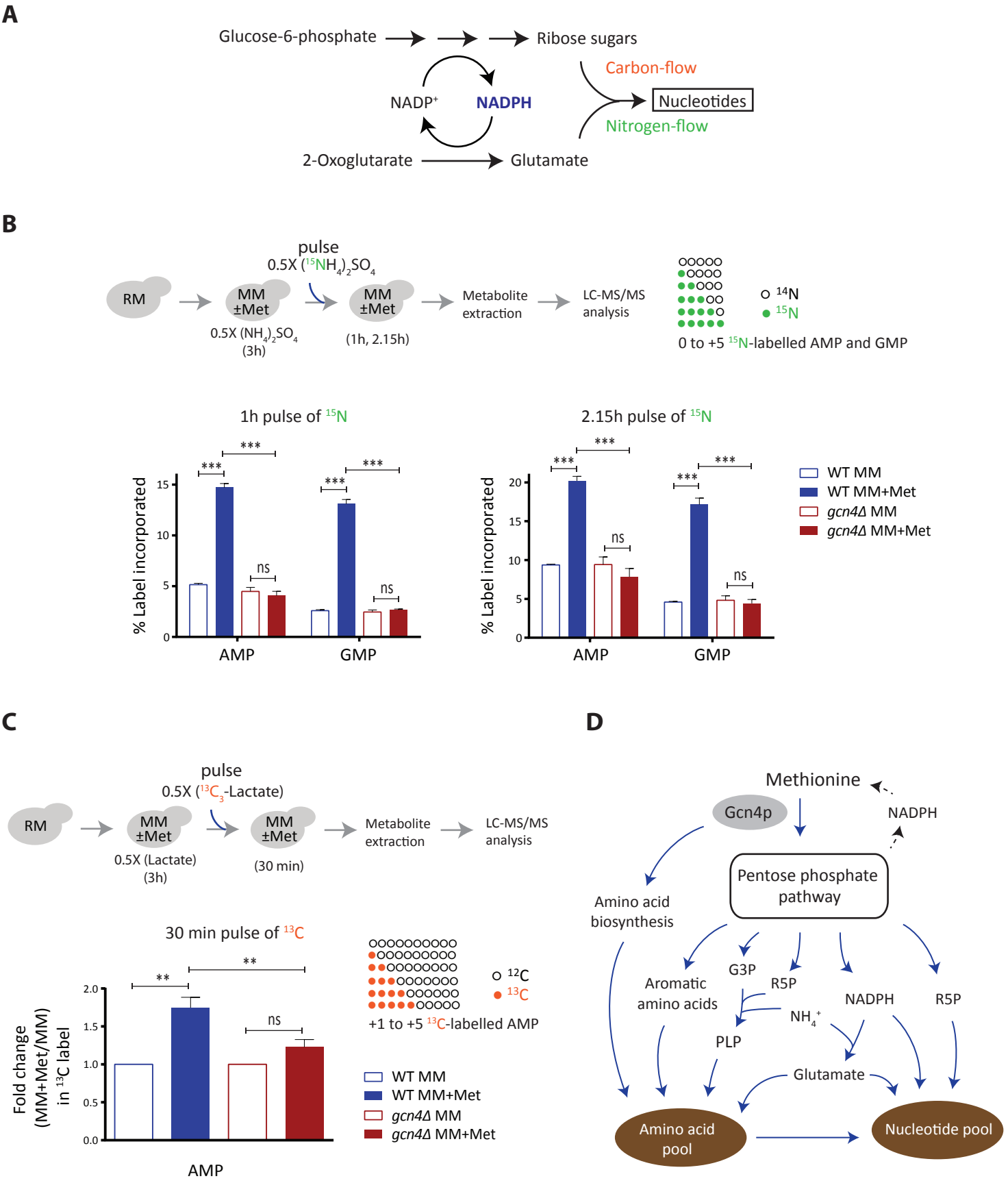
A
Glucose-6-phosphate
Ribose sugars
Carbon-flow
NADP+
NADPH
Nucleotides
Nitrogen-flow
2-Oxoglutarate
Glutamate
B
pulse
0.5X (15NH4)2SO4
RM
MM ±Met
0.5X (NH4)2SO4 (3h)
MM ±Met
(1h, 2.15h)
Metabolite extraction
LC-MS/MS analysis
14N
15N
0 to +5 15N-labelled AMP and GMP
1h pulse of 15N
2.15h pulse of 15N
% Label incorporated
AMP
GMP
***
ns
WT MM
WT MM+Met
gcn4Δ MM
gcn4Δ MM+Met
C
pulse
0.5X (13C3-Lactate)
RM
MM ±Met
0.5X (Lactate) (3h)
MM ±Met
(30 min)
Metabolite extraction
LC-MS/MS analysis
30 min pulse of 13C
Fold change (MM+Met/MM) in 13C label
AMP
**
ns
12C
13C
+1 to +5 13C-labelled AMP
WT MM
WT MM+Met
gcn4Δ MM
gcn4Δ MM+Met
D
Methionine
Gcn4p
NADPH
Pentose phosphate pathway
Amino acid biosynthesis
Aromatic amino acids
G3P
R5P
NH4+
NADPH
R5P
PLP
Glutamate
Amino acid pool
Nucleotide pool